Delft University of Technology
Faculty of Applied Sciences
Faculty of Electrical Engineering, Mathematics and Computer Science

Optimizing the gradient ring of a low-field MRI scanner

By:
A.E. Meijer

Bachelor Final Project
BSc Applied Mathematics
BSc Applied Physics

Supervisors: Dr.ir. M.B. van Gijzen
Dr. K.W.A. van Dongen
Delft, the Netherlands

August 27, 2019

Abstract

This report describes the study on the optimization of the magnetic field generated by a low-field magnetic resonance imaging modality. This modality consists of an outer gradient ring of 36 magnets enclosing a magnet cylinder of four rings with inner gradient and shimming rings.

To obtain the optimal orientation of all 36 magnets in the outer gradient ring, a discrete Genetic Algorithm is used. For each 1-inch N52 NdFeB cube magnet (with a remanence of 1.465 T) it is determined whether or not it is present in an optimal gradient ring. The Halbach orientations are considered as a starting position. The Genetic Algorithm is repeated several times for the first four Halbach orders. Besides this discrete method, a continuous quasi-Newton Algorithm, the fminunc algorithm, is used to optimize the angles of the magnetization of the magnets. For this optimization, all magnets are present. To obtain a greater understanding of the magnetic field generated by the magnet cylinder and the outer gradient ring, the magnetic fields of these objects are simulated, measured and compared.

From the discrete and the continuous optimizations it follows that the N52 magnets used in the initial outer gradient ring could be used if not the entire magnet ring is filled. The best optimizations using the Genetic Algorithm are done when applying a volume correction factor an using a first order Halbach configuration. The resulting mean relative error of the field with respect to the desired field of the generated magnetic field of the outer gradient ring is 8.3%, with a mean relative error slightly smaller than 7.8% for the optimal configuration. Using the fminunc algorithm results in a mean relative error in the field of 33%, with a mean relative error of 32% for the most optimal configuration. The results of the fminunc algorithm are not converging to one optimal solution and the errors are quite big. This is because the magnets used are not suitable for filling an entire gradient ring and obtaining the desired magnetic field at the same time. The magnetic remanence of these magnets is too large for that. The Genetic Algorithm shows that the magnets might be useful if only half of the magnets are used in the gradient ring.

A way of improving the outer gradient ring is to optimize the ring while taking into account more directions per magnet in the Genetic Algorithm. In this report in every optimization of the Genetic Algorithm only one direction is taken into account. The direction taken into account differs per optimization, but it would be useful to consider all these directions in one optimization.
Another way of improvement could be using the quasi-Newton Algorithm with magnets with a different magnetic remanence or a different size. Weaker or smaller magnets would probably be more suitable to use in a completely filled ring.

Preface

About a year ago, I was looking for a Bachelor Final Project in order to fulfill the final requirements of the Bachelors of Science Applied Mathematics and Applied Physics. The project I was looking for should consist for approximately 50% of mathematics and 50% of physics. When I encountered this project, I was immediately interested and fascinated. Both the mathematical and physical aspect of the project appealed to me and the opportunity to use the gifts I have received to help others was one of my main reasons to choose this project.

I have a lot to be thankful for and I am grateful for all the great people I have met during this past year of doing research.
First of all, I would like to thank both my supervisors. Martin van Gijzen, you were a true inspiration for me in your enthusiasm for this project and its meaning in our search for the 'low-cost, high-duty' MRI scanner. Your encouraging words were always welcome and I have enjoyed our talks over the year. I am thankful to have had you as my daily supervisor. Koen van Dongen, a bit more on the background, but nonetheless of great value for my project. I thank you for giving constructive feedback on my research and for valuing the physical aspects of the research, that was very important to me. Your ability to look critically at the results is really worth pursuing.
Furthermore, I have a lot of people to thank. Thank you, Rob Remis, for explaining your MATLAB program to me, it was invaluable. Tom O'Reilly, you were indispensable, thank you so much for explaining all the things I needed and was interested in concerning the magnets in Delft and Leiden, you taught me a lot. The credits of the measurements go to you. Besides this, I have the entire group of researchers in Delft and Leiden to thank for welcoming me in their team. It has been a wonderful time looking for answers with you.
Last but not least, I would like to thank the people dearest to me, Willem-Jan, my parents, friends and family. Thank you all for being supportive and having confidence in me in this project and Pieter, thank you for helping me improve my MATLAB skills, that was not otiose.

There is a lot I am very grateful for, especially the opportunities I have received, to study, to do this project, to meet the people I have met, to use the talents that are given to me, to learn how to live the life that is meant for me and there is only One to thank for all of these blessings. So, I thank the One who is most important to me in life for everything He has given to me. The One who teaches me that everything I do in my life only has value if it is done for Him and if it is done in love.

Angeline Meijer
Delft, August 2019

Contents

1 Introduction

Nowadays, in the Netherlands and other Western countries it is common practice to use advanced medical imaging techniques. One of these techniques is magnetic resonance imaging (MRI). MRI systems are relatively standard in hospitals in the relatively rich part of the world. In the Netherlands there were 10.4 MRI systems per million citizens in 2009, [1]. Using MRI, several illnesses and injuries can be detected very fast and accurate allowing treatments to be started in time.

However, in developing regions, like West Africa, systems for magnetic resonance imaging are definitely not standard. In 2018, 84 MRI machines served 372.551.411 citizens in West Africa. The country with the highest rate of MRI units per million people was Ghana with a rate of 0.48 machines per million people, [2]. In these countries some illnesses are often diagnosed too late. One such illness is hydrocephalus, which occurs all over the world. In developed countries, hydrocephalus can be diagnosed very early in a child's life and usually it can be resolved. However, in developing countries, this illness is often detected too late, so relatively many children suffer from hydrocephalus, [3].

To find a solution for this, teams from all over the world work together to find opportunities to improve this situation. A team of researchers from Delft University of Technology, Leiden University Medical Center and Pennsylvania State University is working on a 'low-cost, high-duty' MRI scanner, an MRI scanner that is relatively inexpensive, but can still be used to detect hydrocephalus. The MRI scanner that is being realized does not, as a regular MRI scanner, use high-amplitude magnetic fields, however, it uses low magnetic field imaging. The low magnetic field is obtained using constructions consisting of several rings with permanent magnets with a certain magnetization, Figure 1. Using

Figure 1: Latest version of the low field MRI-scanner prototype that is made in Leiden [4].

low magnetic fields however implies some difficulties that have to be addressed before the magnet is suitable for usage in MR imaging. One such difficulty is the inhomogeneity of the magnetic field in the magnet. The employed field should be as homogeneous as possible, but in the mean time still have variations in order to ensure that the signal that is received can be traced back to a location in the magnetic field (spatial encoding), [5].

The goal of this project is to do research after and try to answer the following research question:

⇒ **How should the magnetic cubes in the outer gradient ring of a certain magnet cylinder be arranged in order to obtain a desired magnetic field inside the cylinder?**

This is done by considering the theory on magnets and magnetic fields, magnetic resonance imaging, Halbach arrays, homogeneity and shimming. In order to determine the orientation of the magnetization of a certain ring in the magnet that generates a desired field, two different optimization algorithms are regarded, the genetic algorithm and a quasi-Newton algorithm. Using these algorithms a program

is written in MATLAB that gives the configuration of the magnetization in the magnets in the ring given a desired magnetic field.

In Chapter 2, the theory on magnets and magnetic fields, magnetic resonance imaging and Halbach arrays is discussed. Next, the research setup used for measuring data and doing simulations is described. Subsequently, the mathematical approach is given, elaborating on the genetic algorithm and a quasi-Newton algorithm. These algorithms are used to optimize a configuration for the magnetization of the ring. After that, the results of several simulations and measurements are given and discussed. Finally, conclusions are drawn and suggestions for further research are made.

This is the report of the Bachelor Final Project, done in the third year of the Bachelors of Science Applied Mathematics and Applied Physics of the Delft University of Technology.

2 Theory

The goal of this project is to do research after the magnetization that magnets in rings should have to obtain a desired magnetic field within a cylinder of rings. In this section of the report, background information and theory of several subjects is given. This is done for the subjects: magnets and magnetic fields, based on [6], MRI, after [7], [8], [9] and [10] and Halbach arrays, based on [6].

2.1 Magnets and magnetic fields

A magnet is an object that generates a magnetic field. This magnetic field is a vector field that characterizes the influence of magnetic materials or moving charges on other (moving) charges or magnetic materials. When looking at magnets there are considered to be three different kinds: permanent magnets, temporary magnets and electromagnets. In this research only the permanent magnets and electromagnets will be considered.

All magnetic materials have microscopically tiny currents of electrons orbiting around nuclei and electron spins. These currents can be treated as magnetic dipoles if they are used for macroscopic purposes. When the material is not magnetized, the magnetic dipoles have an arbitrary direction and thus cancel each other out, this can be seen in Figure 2a. Magnets are objects that produce a constant magnetic field when they are magnetized. What happens when a material is being magnetized is that the magnetic dipoles align parallel or anti-parallel to the external magnetic field. Most of the moments will align parallel to the field as this is a lower energy state than the anti-parallel orientation. Thus, the material will obtain a net alignment, this can be seen in Figure 2b.
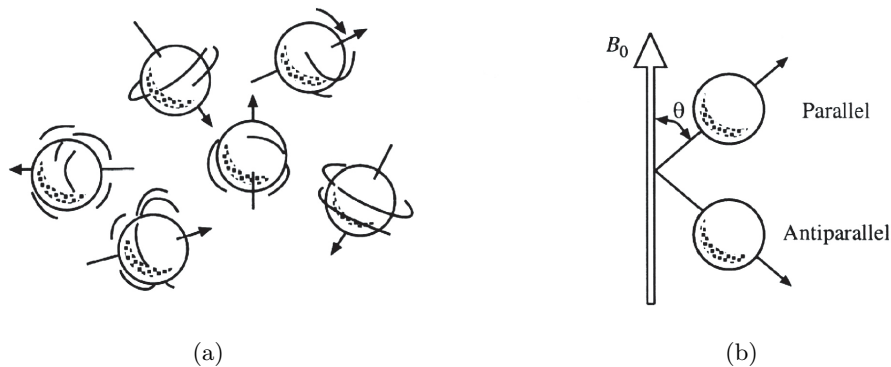

| (a) | (b) |

Figure 2: a) Magnetic moments, without an externally applied magnetic field, having a random orientation. b) Magnetic moment within an externally applied magnetic field B_0, aligning parallel or anti-parallel, [11].

This net alignment is called the magnetic moment, $\mathbf{m}$, of the material. This is a quantity that represents the magnetic strength and orientation of a magnet or other magnetic field inducing object. Another important quantity in magnetized materials is the magnetization, a vector of which the length represents the amount of magnetic dipoles per unit volume and of which the direction is the orientation of the magnetic dipoles. The magnetization is linked to the magnetic moment in the following way

$$\mathbf{M} = \frac{\mathrm{d}\mathbf{m}}{\mathrm{d}V}, \tag{1}$$

where $\mathbf{M}$ is the magnetization, $\mathbf{m}$ is the magnetic moment and $\mathrm{d}V$ is the volume element.

The difference between temporary and permanent magnets is that a temporary magnet cannot keep (a part of) its magnetization without an externally applied magnetic field, while a permanent magnet can. The magnetization that remains in the permanent magnet after the magnetic field that has magnetized the material is removed is linked to a new property, the residual magnetic flux density. This residual magnetic flux density is also called remanence. This link can be seen in

$$\mathbf{B_r} = \mu_0 \mathbf{M_r}, \tag{2}$$

where $\mathbf{B_r}$ is the magnetic remanence in T, μ_0 is the vacuum permeability in $\mathrm{m\,kg\,s^{-2}\,A^{-2}}$ and $\mathbf{M_r}$ is the magnetization in $\mathrm{A\,m^{-1}}$ that remains in the magnet without any external magnetic field. Because of this remanence the object will induce a magnetic field. This magnetic field can be calculated using

$$\mathbf{B}(\mathbf{r}) = \frac{\mu_0}{4\pi} \int \frac{3\mathbf{q}(\mathbf{r}, \mathbf{r}')[\mathbf{q}(\mathbf{r}, \mathbf{r}') \cdot \mathbf{M}(\mathbf{r}')] - \mathbf{M}(\mathbf{r}')}{|\mathbf{r} - \mathbf{r}'|^3} d\tau', \tag{3}$$

where $\mathbf{B}(\mathbf{r})$ is the magnetic flux density on position $\mathbf{r}$ in space, μ_0 is the magnetic permeability in vacuum, $\mathbf{M}(\mathbf{r}')$ is the magnetization at location $\mathbf{r}'$ in the material and $\mathbf{q}(\mathbf{r}, \mathbf{r}') = \frac{\mathbf{r} - \mathbf{r}'}{|\mathbf{r} - \mathbf{r}'|}$. Thus the magnetic flux density is calculated by calculating a volume integral over the magnetized material. The derivation of (3) is given in Appendix A.1.

The other kind of magnets that are considered are the electromagnets. These magnets create a magnetic field when electric current passes through them. When the current stops flowing, the magnetic field vanishes.
A special kind of electromagnets is the superconductor. If superconducting material is cooled down to a certain low temperature (this temperature depends on the material) its resistance will vanish. In that case a current could flow through a superconducting loop infinitely long if the material stays in the same state. The magnetic field a superconductor can induce is relatively large since very high currents can flow through the wires. This magnetic field can be calculated using the Biot-Savart law:

$$\mathbf{B}(\mathbf{r}) = \frac{\mu_0}{4\pi} I \int \frac{d\mathbf{l}' \times \hat{\mathbf{r}}^*}{(r^*)^2}, \tag{4}$$

where (4), $\mathbf{B}(\mathbf{r})$ is the magnetic field on position $\mathbf{r}$, I is the current through the wire, $d\mathbf{l}'$ is a line segment of the wire with the direction of its orientation and $\hat{\mathbf{r}}^*$ is the unit vector of the vector $\mathbf{r}^*$ from the line segment $d\mathbf{l}'$ to the position $\mathbf{r}$, see Figure 3. In the figure $\mathbf{r}^*$ is represented by script letter r.
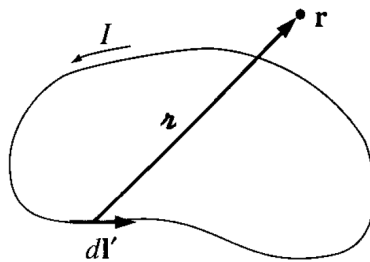

Figure 3: The properties in the Biot-Savart law, (4), indicated, [6].

2.2 Magnetic Resonance Imaging

In Magnetic Resonance Imaging (MRI) systems, different techniques can be used in order to obtain an image. In the scope of this report, only low and high-field MRI are of interest. These terms refer

to a high ($>$1.0 T) respectively low ($<$0.3 T) magnetic field strength. MR systems consist of three parts: the main magnet, the radio frequency (RF) system and the gradient. In the following section, a process that takes place in MRI is discussed. After that, the specifics of high-field and low-field MRI is presented.

2.2.1 The principles of MRI

In MRI the property that an object, in this case a (part of the) human body, can be magnetized using magnetic fields is utilized. Hydrogen is present in fat and in water and thus in large parts of the body the magnetization of hydrogen can be used to image these parts of the body. The hydrogen nucleus, which exists of only one proton and has spin, acts as a magnetic dipole. Thus the nucleus of hydrogen has a magnetic dipole moment and thus has an orientation. When no magnetic field is present, the orientations of the hydrogen protons are random. The orientation of the nucleus of hydrogen is the same orientation of the spin of the nucleus.

2.2.2 The main magnet

What happens when the MRI system is turned on is that a magnet generates a constant large magnetic field, referred to as $\mathbf{B_0}$. This magnet is the main magnet. When $\mathbf{B_0}$ is turned on, all the spins in the hydrogen nuclei align parallel or anti-parallel to $\mathbf{B_0}$, with the majority aligning parallel to $\mathbf{B_0}$, as in Figure 2.

2.2.3 The radio frequency system

Till now, the situation looks static, but this is not completely true. All particles with non-zero spin precess in a constant external magnetic field, [12], in our case the $\mathbf{B_0}$-field. This, however, is not visible yet since the spin and the precession are in the same direction. Now the radio frequency (RF) system becomes of use. The RF system contains two coils, a transmitter coil and a receiver coil. First, the transmitter coil emits a rotating magnetic field $\mathbf{B_1}$ by alternating the current through the coil. The energy of this field is absorbed in the body and with that absorbed energy spins are excited to a higher-energy state and deflected from their initial orientation since the $\mathbf{B_1}$-field is perpendicular to $\mathbf{B_0}$. The spins precess at Larmor frequency, so also $\mathbf{B_1}$ rotates near the Larmor frequency, since then the energy transfer between $\mathbf{B_1}$ and the spins is most efficient. This rotating magnetic field exists only for a short time, 2×10^{-5} seconds. After the $\mathbf{B_1}$-field has vanished, the spins, again precessing around $\mathbf{B_0}$ but still deflected from their initial orientation, then relax to an orientation parallel or anti-parallel to $\mathbf{B_0}$ by releasing their energy to their surroundings. This relaxation, seen from the laboratory frame, can be seen in Figure 4.
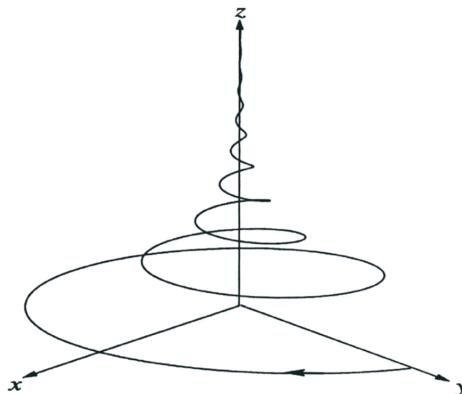

Figure 4: Relaxation of the spin in the laboratory frame when B_0 is in the z-direction.

During this entire process after the $\mathbf{B_1}$-pulse resonance occurs, since the net magnetization, $\mathbf{M}$, precesses. Since the net magnetization precesses, also the net magnetic flux oscillates. This oscillation of the net flux induces a current in the receiver coil. From this current information about the frequency and phase of the current is extracted. The speed with which the spins converge to their $\mathbf{B_0}$-aligned orientation depends on the material.

2.2.4 The gradient

As said, the MR system also contains a gradient, what is this gradient for? The frequency of precession of the protons depends on the strength of the magnetic field. Thus, if there is an inhomogeneous field, the precession frequencies and thus the resonant frequencies vary as a function of position. So, if the variation in the magnetic field is linear, or any other monotonic increasing or decreasing field, each spot in the scanner has a different resonant frequency. Thus, when the receiver coil receives a signal with a certain frequency, it can be traced back from where that signal was generated. Thus variations in the field can be used for spatial encoding. The gradient is used to obtain these variations in the field. The maximum gradient field strength that the MR system can handle is dependent on the receiver bandwidth, as can be seen in

$$G_x = \frac{B_{width}}{FOV_x \gamma}, \tag{5}$$

where G_x is the maximum allowable gradient in the x-direction, B_{width} is the receiver bandwidth, FOV_x is the field of view in the x-direction and $\gamma = 42.6 \times 10^6$ Hz is the gyromagnetic ratio for hydrogen.

2.2.5 High-field MRI

Introducing high-field and low-field MRI, what is so specific about high-field MRI? In high-field MRI also the three parts of the MR system are present, but they might look different than those in low-field MRI. In high-field MRI, the main magnet is made of superconducting material, this is typically used in 3 Tesla (T) or 7 T MRI systems. The superconducting material has to be cooled, most of the time liquid helium is used. Especially the utilization of liquid helium is what makes this MRI system so expensive. The RF-system that is described above, with a transmitter and a receiver option can be used in both high- and low-field MRI, however, nowadays in high-field MRI it is more common to use separated transmitter coils and receiver coils. How the gradient is applied in high-field MRI is as follows, there are three different gradients, in the x-, the y- and the z-direction. Each of these gradients can be obtained by using a certain gradient coil. These three different gradient coils can be seen in Figure 5. In these figures, the positive x-direction is defined horizontally to the right, seen from the cylinder axis, the positive y-direction is defined in the vertical direction, seen from the cylinder axis and the positive z-direction is defined in the direction of the cylinder axis.
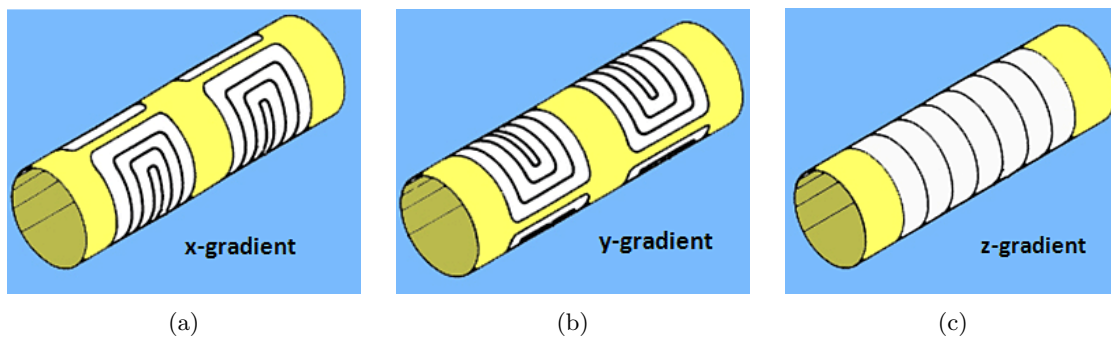

| (a) | (b) | (c) |

Figure 5: a) Gradient coil for the x-gradient. b) Gradient coil for the y-gradient. c) Gradient coil for the z-gradient.

2.2.6 Low-field MRI

Instead of using a superconductor as in high-field MRI, low-field MRI commonly makes use of other electromagnets or permanent magnets. When using electromagnets a disadvantage is that cooling is still needed, since heat will be generated in the magnets because of the resistance. Another disadvantage is that a constant power supply is needed. This makes this MRI option quite expensive.

The last option is to use permanent magnets. The advantage is that permanent magnets have a constant, predictable magnetic field and when using these magnets no current is needed to obtain their magnetic field. So the maintenance of an MR system with permanent magnets is very inexpensive relative to the other options. The main drawback here is that magnets are quite heavy and in order to obtain higher field strengths, the magnet will become considerably heavier.

In low-field MRI the RF-system is as described in Section 2.2.3, so an RF-coil with both transmitter and receiver setting.

The gradient coils described in Section 2.2.5 can also be used in low-field systems. A disadvantage is that this also needs a constant power supply, so again the other option is to apply a gradient using permanent magnets. This will again add weight, but has the same advantages as the main magnet made of permanent magnets, namely the predictability, consistency and cheapness of these magnets.

2.3 Halbach cylinder

A Halbach cylinder is an infinitely long magnetized cylinder made of a material with a continuous transition of magnetization. The strength of the magnetization is constant all over the cylinder and its direction depends on the angle θ. In this ideal case the magnetic field generated by the cylinder lies completely within it, with no magnetic field outside it at all.

Halbach cylinders exist in different orders, the angle of the magnetization in the cylinder also depends on the order of the Halbach array. Everywhere in the cylinder the remanence is given as follows:

$$\begin{cases} B_{x,r} = B_r(\cos(n\theta)\cos(\theta) - \sin(n\theta)\sin(\theta)) \\ B_{y,r} = B_r(\cos(n\theta)\sin(\theta) + \sin(n\theta)\cos(\theta)). \end{cases} \quad (6)$$

Here $B_{x,r}$, $B_{y,r}$ and B_r are respectively the remanence in the x-direction, the remanence in the y-direction and the total remanence of the magnet, this last one is a material property, all in T. Furthermore, n is the order of the Halbach cylinder, which is dimensionless, and θ is the angle in radians, in Figure 6 is indicated how θ is defined.
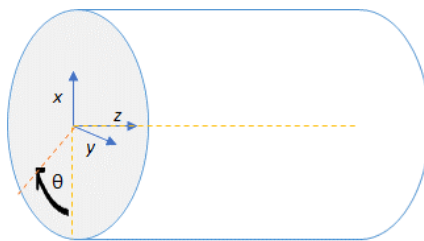

Figure 6: Halbach cylinder with definition of the x-, y-, z- and θ-direction.

In Figure 7, the first two orders of the Halbach orientations are given with the magnetic fields they generate.
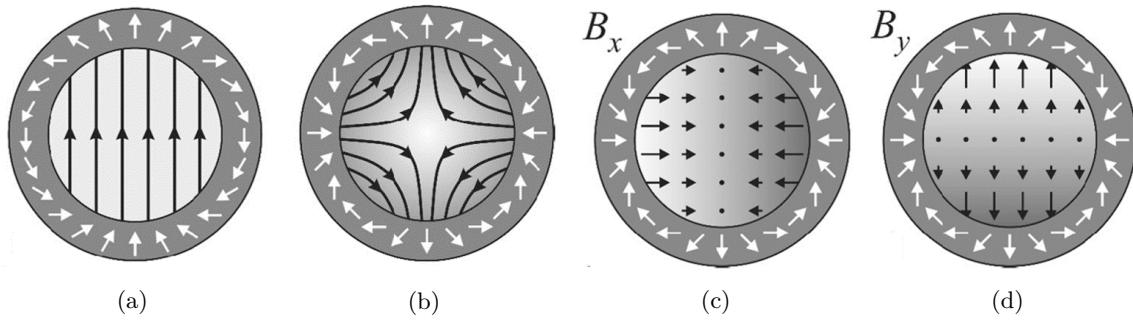
Figure 7: a) First order Halbach configuration with inside the ring the magnetic flux density given. b) Second order Halbach configuration with inside the ring the magnetic flux density given. c) Second order Halbach configuration with inside the ring the magnetic flux density in the x-direction, B_x, given. d) Second order Halbach configuration with inside the ring the magnetic flux density in the y-direction, B_y, given.

In Section 3.1, the use of Halbach cylinders in MRI is discussed.

3 Research Setup

In this research on the configuration of certain rings in a setup, first the magnets and rings that are considered are specified, the entire setting of the magnets is explained in this chapter. The magnet that is used for the measurements, the simulations and the optimizations consists of three parts, the magnet cylinder, the already implemented gradient and shimming rings within the cylinder and a gradient ring around the cylinder. In order to limit the research, the first two parts will be fixed and the last part, the configuration of the magnetization on the gradient ring around the cylinder will be considered in later chapters. The magnetic fields that all the magnets generate is simulated in Chapter 5: Measurements.

3.1 Magnet cylinder

The first part of the magnet consists of the magnet cylinder which is the core part of the magnet. The cylinder consists of four rings with in each ring 24 1-inch cube magnets NdFeB N52 magnets. The residual flux density, B_r, of these magnets is between 1.45 and 1.48 T, [13]. These magnets are put into a first order Halbach configuration. Since the configuration is a *Halbach* configuration, the field strength inside the rings is maximized while the field outside is minimized and tends to go to zero relatively quick. Furthermore, a *first order* Halbach configuration is used since this would ensure a homogeneous magnetic field in the case of an ideal Halbach cylinder. Of course, in this case the situation is far from ideal, though. One ring is not an infinitely long cylinder and the magnetization of the ring is not continuous but discretized in 24 distinct magnets. This results in the magnetic field of the magnet not being completely homogeneous. The four rings in the cylinder all have the same configuration and the same inner radius of 0.150 m. They are positioned 0.0246 m apart. In Figure 8, the cylinder and the configuration of the rings are given.
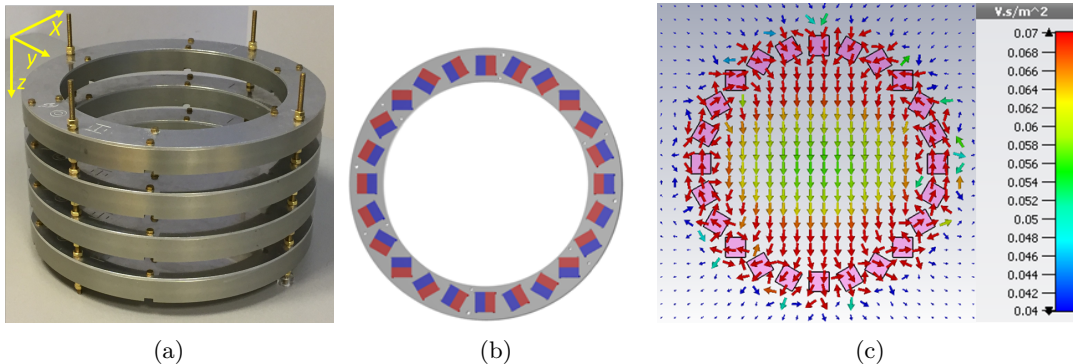

(a) (b) (c)

Figure 8: a) Cylinder positioned at Delft University of Technology, consisting of four rings. b) Configuration of the 24 1-inch cube magnets. c) Simulated magnetic field resulting from the ring in 8b.

The magnetic field in the z-direction that the rings generate is in the order of 10^{-18} T, and hence negligible, even in the non-ideal case.

3.2 Implemented gradient and shimming rings

To obtain a more homogeneous field, two extra magnet rings are inserted in the cylinder. These rings are called shimming rings. Both shimming rings are of a first order Halbach configuration, with magnets removed at 0° and 180°, as can be seen in Figure 9. The first shimming ring consists of 20 magnets and has a radius of 0.0830 m. The second shimming ring consists of 6 magnets and has a radius of 0.060 m. The magnets that are used in these shimming rings are 12 mm NdFeB N48 cubes

that have a B_r in the range of 1.37-1.42 T, [14]. Both rings are placed 0.0827 m outside the centre of the z-axis of the magnet.
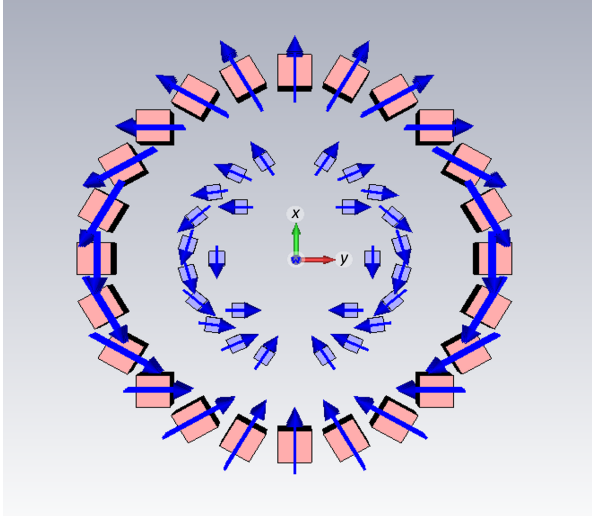

Figure 9: A cylinder ring with the inserted shimming rings. The most outer ring represents a ring from the cylinder as in Figure 8, the two rings within this ring are the shimming rings.

Besides the shimming ring also inner gradient rings are added in order to obtain a gradient of the field. The gradient rings are three identical rings combining 16 NdFeB N42 5 mm cube magnets. The strength of these magnets is weaker than that of the other magnets used till now; B_r is between 1.29-1.32 T, [15]. The radii of these rings are 0.0905 m and the rings are placed 0.050 m apart from each other. The magnets in these rings are ordered in an adjusted version of a first order Halbach ring orientation. Some magnets have an orientation that is rotated over 180°, as can be seen in Figure 10.
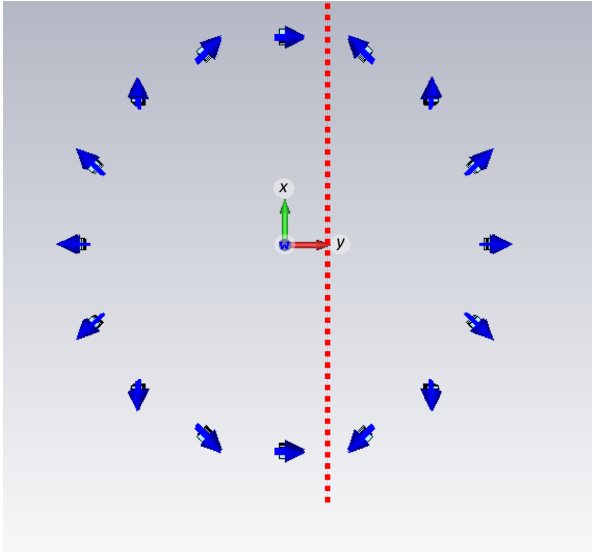

Figure 10: The inner gradient ring that can be installed in the cylinder. The red line indicates the separation between the magnets in the normal Halbach configuration and the magnets that have a Halbach configuration rotated over 180°.

3.3 Outer gradient ring

One way the cylinder just described in the previous sections could be used for MRI purposes is to add a strictly monotonic gradient to the field. This gradient would provide for spatial encoding. In order to obtain such a strictly monotonic gradient another gradient ring is added outside the magnet cylinder. From literature, [5], it is known that the magnets in this gradient ring should have a second order Halbach orientation if inside the cylinder the field would be homogeneous. Thus, for a first approximation this second order Halbach orientation is implemented in the outer gradient ring. For this gradient ring, 36 1-inch cube NdFeB N52 magnets are used, the same as for the cylinder in Section 3.1. Thus, here B_r is again between 1.45 and 1.48 T, [13]. The radius of this ring is 0.175 m. This initial outer gradient ring can be observed in Figure 11.

Figure 11: Outer gradient ring existing of 36 1-inch cube NdFeB N52 magnets in a second order Halbach configuration with a radius of 0.175 m.

However, the field within the cylinder is *not* homogeneous. That is why this research is done, to find out whether there is a more optimal orientation of the magnetization over this outer gradient ring.

3.4 Measuring magnetic fields

Finally, it is desirable to be able to compare the simulations of the magnetic field generated by the final setup, see Figure 12, with the reality. Therefore, the magnetic fields of three different setups are measured, the cylinder including shimming rings, the cylinder including shimming and inner gradient rings and the outer gradient ring. For the measurements a Gaussmeter Model GM 2 from Alphalab Inc. is used. This is a meter that can measure strong and moderate magnetic fields using a probe with an accuracy of $1{\times}10^{-5}$ T. The uncertainty in the temperature range that is measured is: 1% of DC reading and +/- 10 counts with 1 count is $1{\times}10^{-5}$ T, [16]. The measurement process is relatively easy. A COSI Measure moves the probe along a preprogrammed route through the 3D space within the cylinder. This COSI Measure, is an open source multipurpose 3-axis robot with very high spacial fidelity; the robot is reliable on a spacial scale of less than a millimeter, [17]. It measures the magnetic flux density in the x-, y- and z-direction every 5 mm. The results of these measurements are presented in Chapter 5: Measurements.
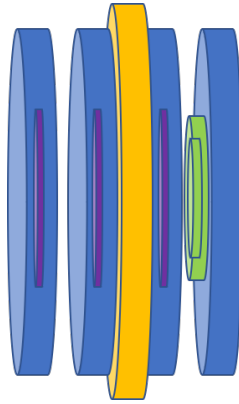
Figure 12: Final setup of the MRI magnet system. The blue rings are the rings from the cylinder described in Section 3.1, the green and purple rings are respectively the shimming and inner gradient rings described in Section 3.2 and the orange ring is the outer gradient ring described in Section 3.3.

4 Mathematical Approach

In order to be able to optimize a ring in the magnet, first the resulting magnetic field of a magnet should be calculated. In this chapter a short introduction to the MATLAB code used to do this is given. Furthermore, to find the optimal configuration of the magnets in the outer gradient ring in order to obtain a desired magnetic field within the magnet cylinder, two algorithms are considered: the discrete Genetic Algorithm (GA) and a continuous quasi-Newton algorithm (QNA). Also these two algorithms will be described in this chapter. All MATLAB code that is described here can be downloaded from `https://drive.google.com/file/d/1_LtmHls6hQagZijoIU91aKMsuKMfjWtR/view?usp=sharing`.

4.1 Simulating magnetic field

The MATLAB code for simulating magnetic fields takes as an input the specifications of the magnet cylinder such as the lengths in the x-, y- and z-direction, the number of discretization cells in these directions, the radii of all rings and where they are positioned, the remanences of all the different magnets in the rings, the number of magnets in the rings and the field of view in which the magnetic field should be evaluated. The scripts first calculates the orientation of the magnetization in the rings and from there using (3) with the composite midpoint rule, the magnetic field is calculated in the observation plane (field of view). This simulation can be done for all rings, the four cylinder rings, the inner gradient and shimming rings and the initial outer gradient ring. Adding these up gives the magnetic field of the total magnet cylinder.

The error, ϵ, of a magnetic field relative to the desired magnetic field is calculated in the following way:

$$\epsilon = \frac{|\mathbf{B_x} - \mathbf{B_{desired}}|}{\mathbf{B_{desired}}}, \tag{7}$$

where $\mathbf{B_x}$ is the magnetic field in the $\boldsymbol{x}$-direction generated by the outer gradient ring and $\mathbf{B_{desired}}$ is the desired magnetic field in the $\boldsymbol{x}$-direction.

4.2 Genetic Algorithm

The Genetic Algorithm, GA, is an algorithm most suited for discrete optimization. Thus the optimization problem should also be discrete. A way of defining the problem is by taking the magnets as the optimization variables, as done in [18]. There the three optimization options are that a magnet spot is empty, filled with an NdFeB N42 magnet or filled with an NdFeB N52 magnet. In this research, however, a few modifications are done. The optimization variables are not taken to be the magnets in the outer gradient ring, but the magnetizations of these magnets.

The goal of the GA here is to find out what orientations of the magnetization the 36 magnets is optimal in order to obtain the desired magnetic field. For each run of the algorithm one magnetization orientation is considered. Thus, the GA has 36 optimization variables. First, the resulting magnetic field for each single magnet for that magnetization orientation is calculated. This results in 36 field maps. Then the total magnetic field of an arbitrary magnet design can be calculated by superposition of all the contributions of the single magnets (the orientation of the magnets that are used in that arbitrary design get the value 1, all other magnets get the value 0). In taking this linear combination, the assumption is done that an individual magnet does not influence the magnetization of the other magnets around it. The GA is used since this is an appropriate algorithm for this non-linear integer problem. The GA is an algorithm that uses the principles of natural selection to minimize the defined fitness function.

The algorithm has several inputs:

1. The fitness function that should be minimized.

2. The Halbach order of the gradient ring that is taken into account.

3. The lower and upper bounds.

4. The optimization options, such as the maximum amount of generations, the maximum running time, the fitness limit, etc.

In this case the fitness function is defined as follows:

$$f_{SEM} = \sum_k \Big(\sum_j \Big(\sum_i \Big((\mathbf{B_{x_{ijk}}} - \mathbf{B_{grad,d_{ijk}}})^2 + \mathbf{B_{y_{ijk}}}^2 + \mathbf{B_{z_{ijk}}}^2 \Big) \Big) \Big), \tag{8}$$

where f_{SEM} is the value of the fitness function, this should be minimized, $\mathbf{B_{x_{ijk}}}$ is the magnetic field in the x-direction in cell (i, j, k) (the space in the magnet cylinder is discretized), $\mathbf{B_{grad,d_{ijk}}}$ is the desired magnetic field of the gradient ring in cell (i, j, k), $\mathbf{B_{y_{ijk}}}$ is the magnetic field in the y-direction in cell (i, j, k) and $\mathbf{B_{z_{ijk}}}$ is the magnetic field in the z-direction in cell (i, j, k). All the magnetic fields are in T. Minimizing the function will give a magnetic field as close to the desired field as possible with the direction of the field everywhere in the x-direction. This last part will ensure that the magnetic field can be used for spacial encoding. Furthermore, this is desirable since the signal model that is used, [7], assumes that the y- and z-component of the magnetic field are 0.

In advance the initial Halbach order of the ring should be chosen. This has impact on the optimization, since for every magnet there are two different magnetization options for the Halbach order chosen: one is the orientation from the chosen Halbach order and the other is a zero magnetisation (when the magnet is left out).

The lower bound for all magnets is chosen to be 0 (magnet not present) and the upper bound for all magnets is set to be 1 (magnet present). Furthermore, all variables are set to be integers, thus forcing the algorithm to choose betwoon 0 and 1 for each magnet.

The optimization options are taken to be the default options from the GA-implementation in MAT-LAB.

4.2.1 Process

How the GA tries to minimize the fitness function will be described in this section, based on [19]. First, the GA generates 200 random magnetization configurations for the 36 magnets (so for every magnet it chooses one of the n possible magnetizations). For these 200 configurations, the value of the fitness function is calculated. Then, a new generation of 200 magnetizations will be generated as follows: 5% will consist of the best 5% configurations of the previous generation (so the 5% configurations that have the lowest values for the fitness function), 75% will be generated by crossover combining the best 5% configurations of the previous generation and 20% will be generated by doing mutations on the best 5% configurations of the previous generation. After this is done, the algorithm runs again and the entire process is repeated. Thus, the optimal magnetization configuration will be found in an iterative way.

4.2.2 Evaluation

There are several advantages and disadvantages of the GA, [20].

First of all, the optimization is very fast because the contributions of all magnetizations of a magnet

can be calculated in advance. Furthermore, an advantage of the algorithm is that it searches a population of configurations in parallel, it does not find a single configuration. Thirdly, only the fitness function and the different configurations need to be given. There is no extra knowledge on derivatives needed, nor other information. Finally, the algorithm uses heuristic and thus probabilistic rules on the generation of new generations, thus it takes all possible configurations into consideration, even the unexpected ones. This can cause strange, but feasible solutions and it reduces the bias in the optimization.

A disadvantage of the GA might be that it does not provide one single optimal solution, but a number of possible solutions to a problem. The final solution is left as a choice to the user. An advantage from this, however, is that the algorithm can be useful in the identification of other optimal solutions, if more than one optimal solution exists.

4.3   Quasi-Newton Algorithm

Since the Genetic Algorithm only takes into account a finite amount of magnetization orientations it is also useful to conduct a continuous optimization for the angles of the magnetizations of each magnet. This is done using a Quasi-Newton Algorithm (QNA) in MATLAB: fminunc.

The fminunc algorithm needs the following inputs:

1. The fitness function that should be minimized.

2. The starting point (starting angle) of the optimization.

3. The optimization options, such as the maximum amount of generations, the maximum running time, the fitness limit, etc.

The fitness function stays the same as in (8), but now the contributions of each magnet can not be calculated in advance, since the magnetization angle is continuous. Thus, the contribution of the magnetization has to be calculated during the optimization. This is done using (3).

In the QNA the starting point for the optimization should be provided. In the GA, this is not needed since the algorithm generates the initial configurations randomly, but in quasi-Newton algorithms this is required since from this point the successive points will be found using gradient-based methods. As starting angle all initial magnetization angles are set to 0°.

The maximum number of iterations is set to 10, because otherwise the running time of the algorithm would be very large. All other optimization options are taken to be the default options from the fminunc-implementation in MATLAB.

4.3.1   Process

The fminunc-algorithm contains two different algorithms that can be applied, the trust-region method and the quasi-Newton method. For the trust-region algorithm the fitness function should include a gradient. Since this is not the case in the fitness function used, the quasi-Newton method is used, [21].

Several gradient-descent algorithms use information about the gradient of the fitness function to find a search direction in which the minimum is expected to be. The easiest way of doing this is defining the search direction as $-\nabla f$, where ∇f is the gradient of the fitness function. However, this method can be quite inefficient and slow.
Quasi-Newton methods can be more efficient. In these methods the information about the slope of the function is build up at each iteration in order to obtain a quadratic model problem looking like this:

$$\min_{\boldsymbol{\alpha}} = \frac{1}{2}\boldsymbol{\alpha}^T \mathbf{H}\boldsymbol{\alpha} + \mathbf{c}^T\boldsymbol{\alpha} + b, \tag{9}$$

where $\mathbf{H}$ is the Hessian matrix, which is positive definite symmetric, given in Equation 10, [22], $\mathbf{c}$ is a constant vector, $\boldsymbol{\alpha}$ is the vector with the optimization variables, the 36 angles of the magnetizations of the magnets and $\boldsymbol{b}$ is a constant.

$$\mathbf{H}_{i,j} = \frac{\partial^2 f_{sem}}{\partial \alpha_i \partial \alpha_j}. \tag{10}$$

The optimal solution for the fitness function is found when the following holds

$$\nabla f_{sem}(\boldsymbol{\alpha}^*) + \mathbf{c} = \mathbf{0}, \tag{11}$$

where $\boldsymbol{\alpha}^*$ is the vector with all the angles of the magnetizations. Thus, the optimal solution can be written as:

$$\boldsymbol{\alpha}^* = -\mathbf{H}^{-1}\mathbf{c}. \tag{12}$$

In order to skip a large amount of computations, the quasi-Newton method does not (as the Newton methods do) calculate the Hessian as in Equation 10. They use an approximation of the Hessian that is calculated using $f_{sem}(\boldsymbol{\alpha}^*)$, $\nabla f_{sem}(\boldsymbol{\alpha}^*)$ and a certain Hessian updating method:

$$\mathbf{H}_{k+1} = \mathbf{H}_k + \frac{\mathbf{q}_k \mathbf{q}_k^T}{\mathbf{q}_k^T \mathbf{s}_k} - \frac{\mathbf{H}_k \mathbf{s}_k \mathbf{s}_k^T \mathbf{H}_k^T}{\mathbf{s}_k^T \mathbf{H}_k \mathbf{s}_k}, \tag{13}$$

where $\mathbf{s}_k = \boldsymbol{\alpha}_{k+1} - \boldsymbol{\alpha}_k$ and $\mathbf{q}_k = \nabla f_{sem}(\boldsymbol{\alpha}_{k+1}) - \nabla f_{sem}(\boldsymbol{\alpha}_k)$. This method is called the BFGS method, [21]. Since the gradient is not analytically given, the partial derivatives are calculated using a finite difference method, this involves giving each optimization variable in $\boldsymbol{\alpha}$ a perturbation and calculating the rate of change in the fitness function, f_{sem}. Furthermore, $\boldsymbol{\alpha}_{k+1} = \boldsymbol{\alpha}_k + u\mathbf{d}_k$. Here $\mathbf{d}_k$ is the search direction given by $\mathbf{d}_k = -\mathbf{H}_k^{-1} \cdot \nabla f_{sem}(\boldsymbol{\alpha}_k)$ and u is the step length parameter, which is a scalar. It is required that the next iteration decreases the fitness function sufficiently, thus, it should satisfy (14), and it is required that the step length is not too small, according to (15)

$$f_{sem}(\boldsymbol{\alpha}_k + u\mathbf{d}_k) \leq f_{sem}(\boldsymbol{\alpha}_k) + c_1 u \nabla f_{sem}^T(\boldsymbol{\alpha}_k)\mathbf{d}_k \tag{14}$$

$$\nabla f_{sem}^T(\boldsymbol{\alpha}_k + u\mathbf{d}_k)\mathbf{d}_k \geq c_2 \nabla f_{sem}^T(\boldsymbol{\alpha}_k)\mathbf{d}_k, \tag{15}$$

where c_1 and c_2 are such that $0 < c_1 < c_2 < 1$ and c_1 and c_2 are constant.

4.3.2 Evaluation

Also using the quasi-Newton algorithm, fminunc, has its pros and cons.

Since the optimization is now described with continuous optimization variables, the fitness function has become continuous too. In this case, gradient methods are the most efficient to use, [21]. Furthermore, by setting the optimization variables to be continuous, all magnetization orientations are considered and not just n options as in the GA.

One main disadvantage of a QNA is that the optimization process takes considerably more computing time than the GA. This is caused by the continuity of the optimization variables, because they are continuous, their contribution to the magnetic field can not be calculated in advance. Besides that, the fminunc optimization algorithm does not guarantee a global optimum, it finds a local minimum.

5   Measurements

The magnetic fields, generated by the magnet rings described in Chapter 3: Research Setup, are simulated using MATLAB and measured using the measurement technique described in Section 3.4. The results are given in this chapter. Only the x-components of the magnetic fields are measured, since all the other components are assumed to be small compared to the x-component.

5.1   Simulated magnet

5.1.1   Magnet cylinder

The first rings that are simulated are the four cylinder ring, since these form the basis of the magnet. In Figure 13 the simulated magnetized ring is shown, this is an approximation of the first order Halbach configuration with 24 magnets, as described in Section 3.1.
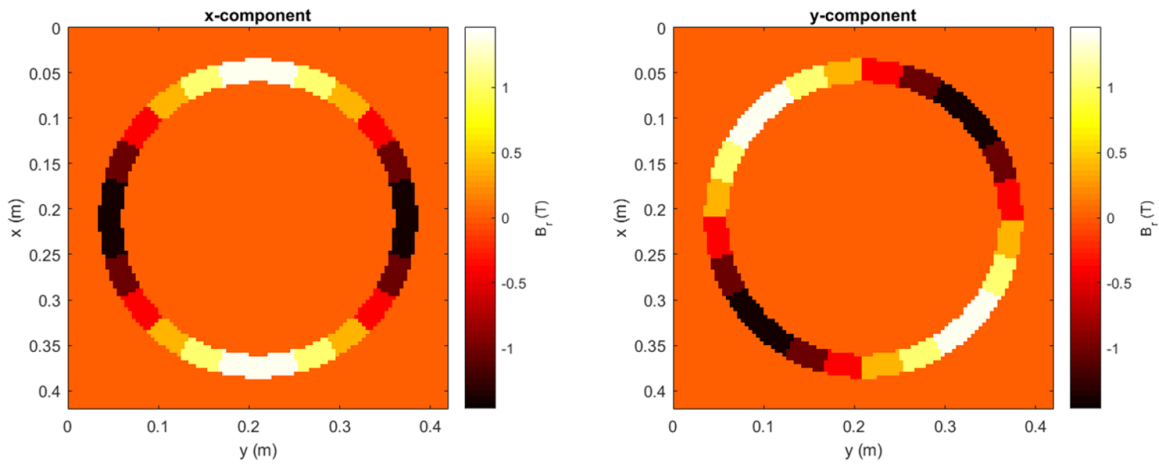

Figure 13: Magnetic remanence, $\boldsymbol{B_r}$, of the four rings in the basis cylinder. On the left, the $\boldsymbol{x}$-component of the remanence and on the right, the $\boldsymbol{y}$-component of the magnetization are given. This configuration is an approximation of the first order Halbach configuration of Figure 7a.

The four rings, as positioned in Figure 12, together with the inner gradient and shimming rings generate the magnetic field shown in Figure 14 in the center of the cylinder. For the optimization the center of the cylinder in the $\boldsymbol{z}$-direction is used.
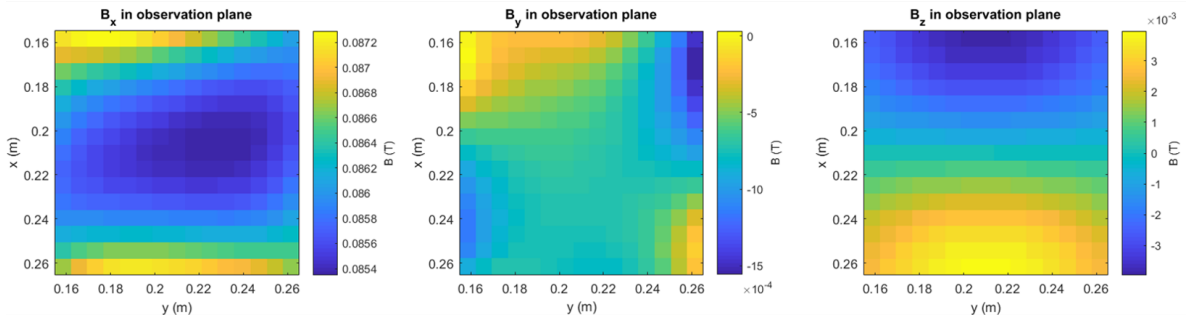

Figure 14: Magnetic field in the middle of the cylinder generated by the four first order Halbach rings with the inner gradient and shimming rings. On the left, the $\boldsymbol{x}$-component of the magnetic field is shown, in the middle, the $\boldsymbol{y}$-component of the magnetic field is shown and on the right, the $\boldsymbol{z}$-component of the magnetic field is shown.

As can be seen in Figure 14, the field does not completely resemble the field of an ideal Halbach, which has a homogeneous field only in the x-direction. The field generated by the magnet cylinder here is not completely homogeneous and there are still y- and z-components of the magnetic field. However, in the figure it can be seen that the y and z-components are much smaller than the x-component and are close to 0 T.

5.1.2 Initial outer gradient ring

From literature, [5], it is given that a second order Halbach cylinder would obtain a linear field inside the cylinder. Therefore, the gradient ring is made in the second order Halbach orientation, this can be seen in Figure 15.
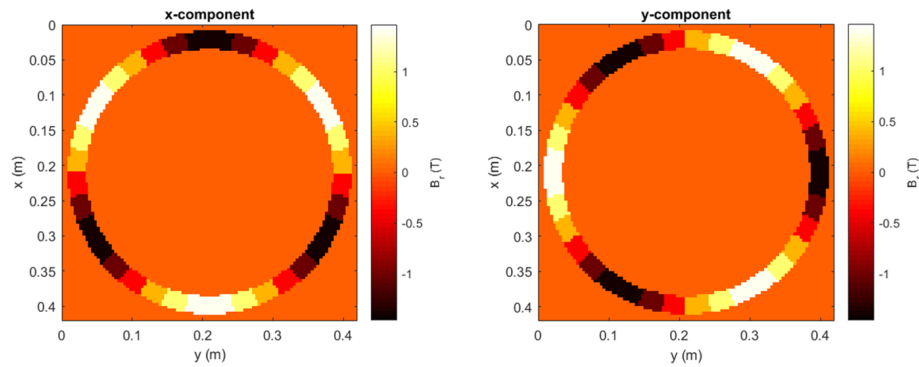

Figure 15: Initial orientation of the outer gradient ring

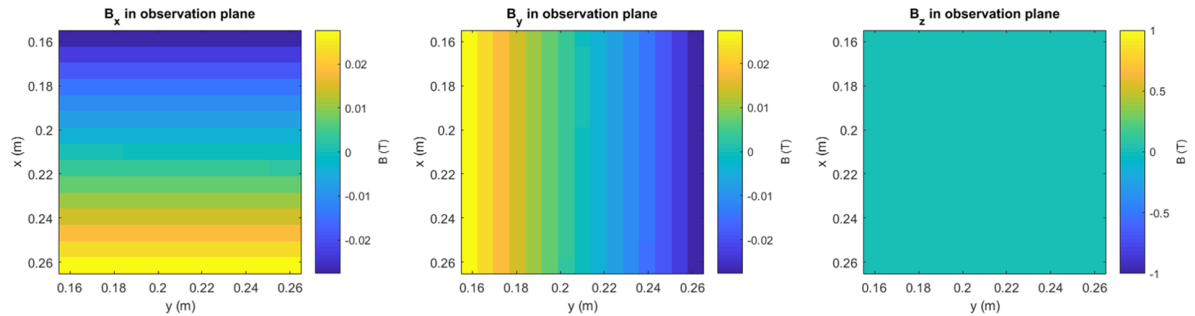The magnetic field that this ring generates is given in Figure 16 and indeed looks linear.

Figure 16: Magnetic field generated by the outer gradient ring with its initial second order Halbach orientation.

The problem with the total field generated from the four ring cylinder and the gradient ring together, Figure 17, is that the gradient that now is incorporated in the field is too large to be used in the MR system, the maximum gradient strength is around 0.010 T/m, as can be calculated from (5) with a receiver bandwidth of 32 kHz and a field of view of 0.10 m. Thus, when looking at a field of view of 0.10 m, the maximum field strength difference would be around 0.001 T over the entire field of view. It can be seen that this difference is approximately 0.010 T, so this is far too large for the current receiver bandwidth.
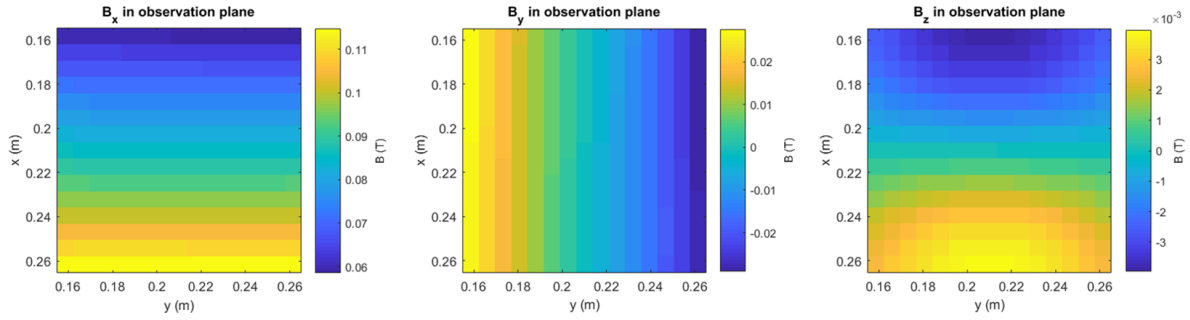
Figure 17: The total magnetic field of the cylinder consisting of four rings and the inner gradient and shimming rings and the initial gradient ring in the x- (left), y- (centre) and z-direction (right).

5.2 Measured magnet

In Figure 18a, the magnetic field in the center of the cylinder is given generated with the four cylinder rings and the shimming rings implemented in the cylinder.
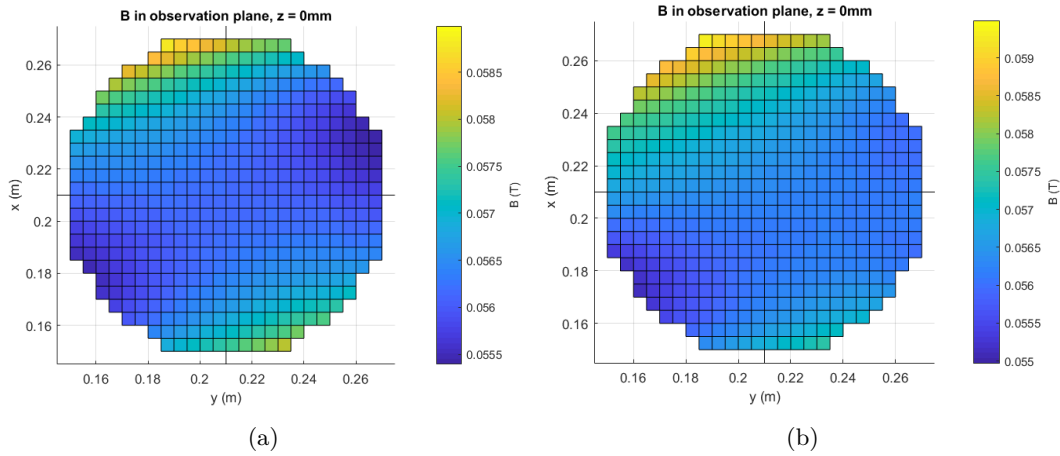

(a)   (b)

Figure 18: a) The measured magnetic field in the x-direction in the center of the cylinder of four rings with the inner shimming rings. b) The measured magnetic field in the x-direction in the center of the cylinder of four rings with the inner gradient and shimming rings.

Furthermore, also the field that is generated by the four cylinder rings with both the shimming rings and the inner gradient rings implemented is measured in the center of the cylinder. This field is given in Figure 18b.
At last, the magnetic field of the initial outer gradient ring is measured in the center of the ring. This resulted in the following field map, Figure 19 on the next page.
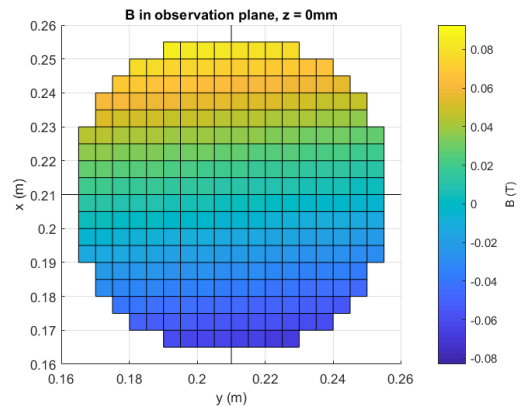
Figure 19: The measured magnetic field in the x-direction in the center of the gradient ring.

6 Optimizations

In this chapter several optimization results will be shown. The optimizations are done using the simulated fields for the magnet cylinder consisting of four first order Halbach rings enclosing the inner gradient and shimming rings as described in the Sections 3.1 and 3.2. Then the outer gradient ring that is described in Section 3.3 will be optimized in order to obtain a certain desired magnetic field within the cylinder. First, the magnetic fields for the cylinder and the initial gradient ring will be given.

6.1 Optimization results

The optimization is done using two different methods, the Genetic Algorithm on a discrete defined optimization problem and the fminunc algorithm (a quasi-Newton Algorithm from MATLAB) on a continuous formulated optimization problem.

In order to be able to optimize the outer gradient ring, first a desired magnetic field is defined within a certain field of view. This desired field is given by the constraints set that the field should be at least of a strength of 0.070 T and it should have a gradient that is at most the gradient calculated in (5), which in our case is 75×10^{-5} T/m. In Figure 20a, the desired linear magnetic field is given, this desired field should be generated by the cylinder with four rings in combination with the outer gradient ring. In order to optimize the ring, the desired field that the gradient ring should generate is calculated by simply subtracting the field of the cylinder, Figure 13, from the desired field, Figure 20a. This field is shown in Figure 20b.
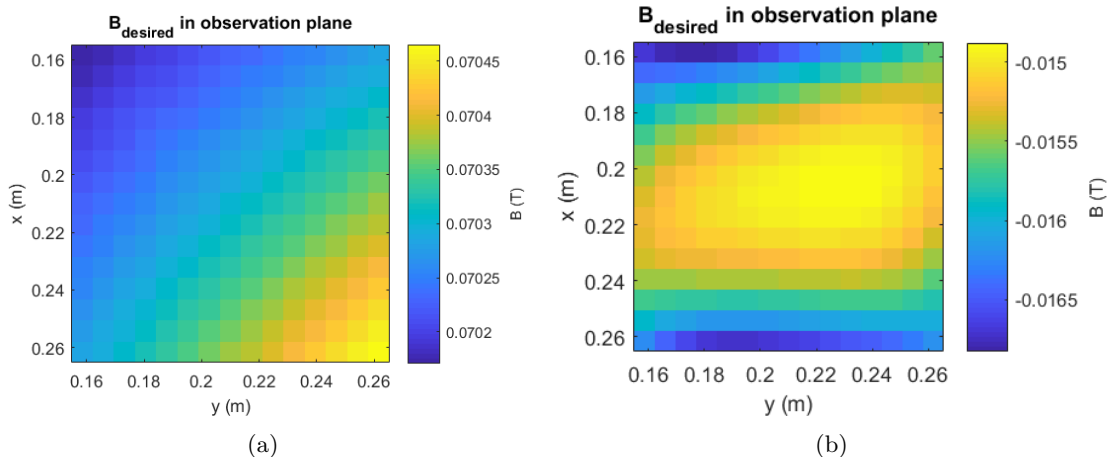

Figure 20: a) The desired magnetic field in T of the cylinder of four rings with the outer gradient ring around it in the observation plane. b) The desired magnetic field in T of the outer gradient ring in the observation plane.

6.1.1 Genetic Algorithm

The Genetic Algorithm is used with taking into account one Halbach order and one orientation at a time, as described in Section 4.2. In this optimization there are two options for each magnet, namely, being oriented in the Halbach orientation or not being present at all. This is done for each of the first four Halbach orientations several times.

The optimization of the field in order to obtain the desired field gives, using the first order Halbach orientation, the result that the outer gradient ring would not be present at all. The mean of

the relative errors of the fields using the second order Halbach orientation is 47% with the best optimization result giving a mean relative error of 46%. Using the third order Halbach orientation, both mean of the optimization runs and the best optimization run give a mean relative error of 28%, so that improves the results a bit. Finally, using the fourth order Halbach orientation gives a mean relative error of 26% with the best result having an error of 25%. So, optimization using the fourth order Halbach configuration is the best option in this case. In Figure 21, the best result of the GA using only one Halbach orientation of a certain order, in this case order four, is given.
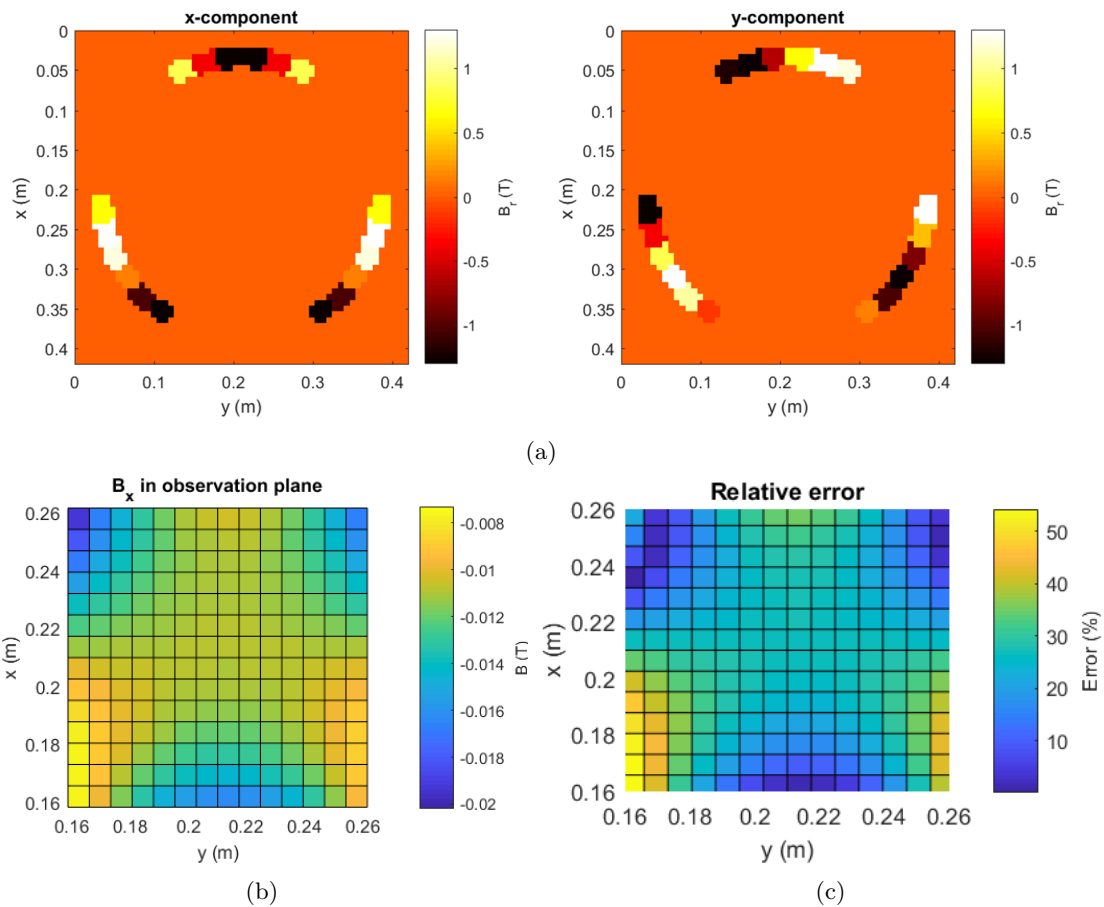

Figure 21: a) The magnetization in the x- and y-direction for the outer gradient ring for the optimized magnetic field using the Genetic Algorithm and a fourth order Halbach orientation on the outer gradient ring. b) The resulting magnetic field in the x-direction. c) The relative error in the resulting magnetic field in the x-direction.

The results the Genetic Algorithm gives for the optimizations differs per Halbach orientation. However, within the orientation, the algorithm converges to solutions that do resemble each other.

6.1.2 Quasi-Newton Algorithm

The fminunc algorithm is run with several starting values for the initial angles of the magnets. The results of these optimizations do not converge to one unique optimal solution. Furthermore, after 11 iterations, using more iterations does not improve the result very much. Starting at the same starting value and using 72 iterations instead of 11 does not make a significant difference for the magnetization and the mean relative error of the solution. In Figure 22a, the result of the algorithm run with 72

iterations is shown and in Figure 22b, the result of the run with 11 iterations is shown.
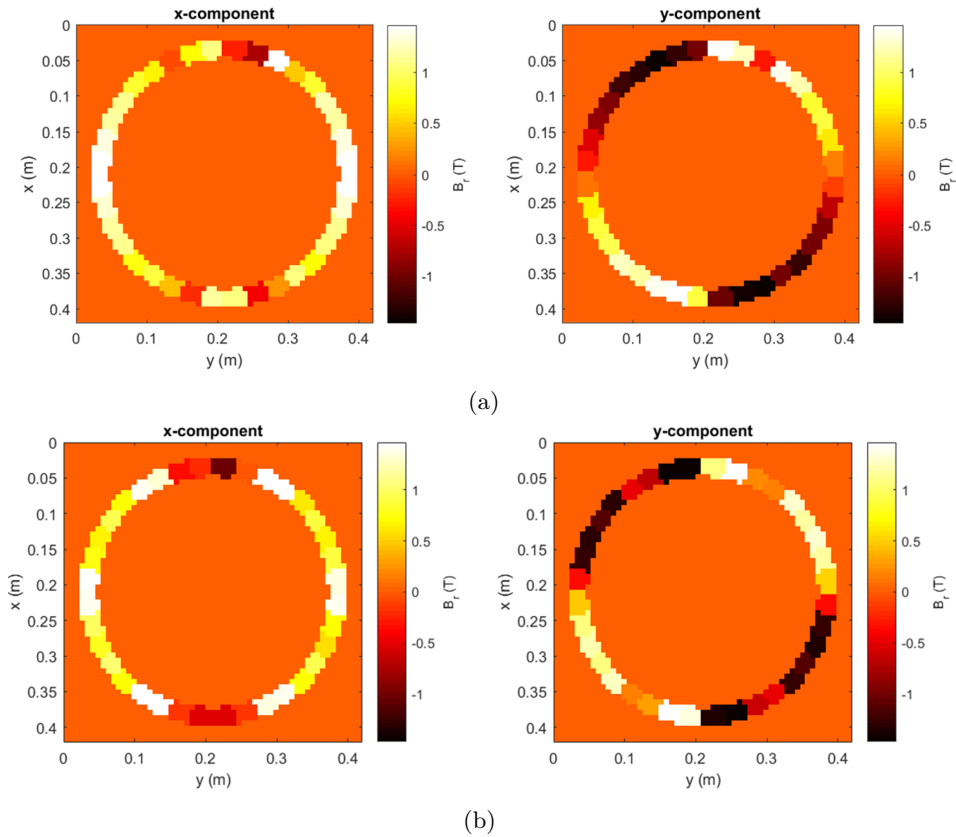

(a)

(b)

Figure 22: a) The magnetization in the $\boldsymbol{x}$- and $\boldsymbol{y}$-direction for the outer gradient ring for the optimized magnetic field using fminunc in 72 iterations. b) The magnetization in the $\boldsymbol{x}$- and $\boldsymbol{y}$-direction for the outer gradient ring for the optimized magnetic field using fminunc in 11 iterations.

The difference between these two configurations is not that large, in Figure 23, the errors relative to the desired magnetic field for the gradient ring are given. It can be observed that the differences between the 72-iteration run and the 11-iteration run are mostly on the sides of the field of view, in the center of the field of view it looks the same.
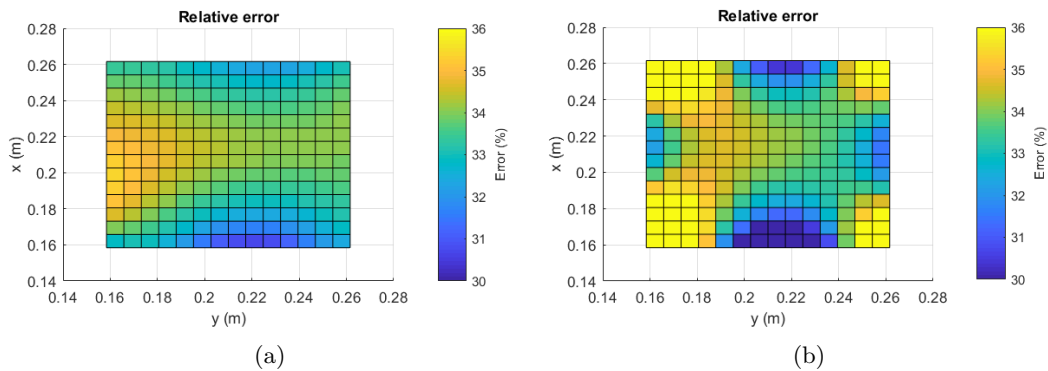

(a)   (b)

Figure 23: a) The relative error of the magnetic field generated by the result of the fminunc algorithm with 81 iterations, Figure 22a. b) The relative error of the magnetic field generated by the result of the fminunc algorithm with 11 iterations, Figure 22b.

The mean relative error of the run with 72 iterations is a bit smaller than 34% and of the run with 11 iterations, this is a bit higher than 34%.

The total of the algorithm runs have an average relative error of 33%. The best run also has a mean relative error of 33%. The results of this run are shown in Figure 24.
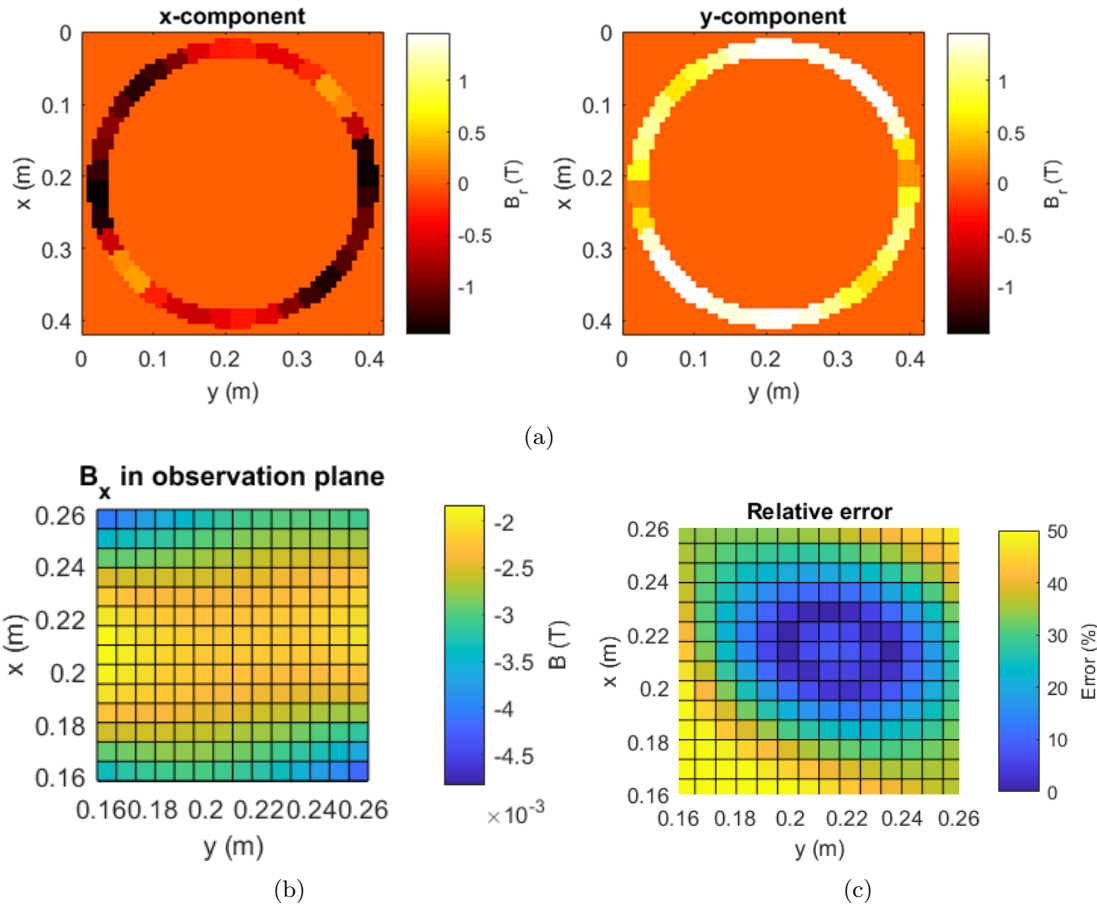

Figure 24: a) The magnetization in the x- and y-direction for the outer gradient ring for the optimized magnetic field using the quasi-Newton method. b) The resulting magnetic field in the x-direction. c) The error in the resulting magnetic field in the x-direction.

7 Discussion

The aim of this research is to optimize a gradient ring in such a way that a desired magnetic field is generated by the ring. In this chapter, the results from the Chapters 5: Measurements and 6: Optimizations will be discussed. First, there will be commented on the results of the optimizations. Then, a comparison will be made between the simulated and the measured magnetic fields of the four ring cylinder and the outer gradient ring.

7.1 Comparison of simulated and measured magnetic field

In section 5.1, the simulated magnetic fields of the four ring cylinder and the outer gradient ring are given in the figures 14 and 16. Furthermore, in Chapter 5: Measurements, of the same objects the magnetic field is measured, with the results in the Figures 18 and 19. The difference between the simulated and the measured magnetic fields are given in Figure 25 for the cylinder and in Figure 26 for the initial outer gradient ring.
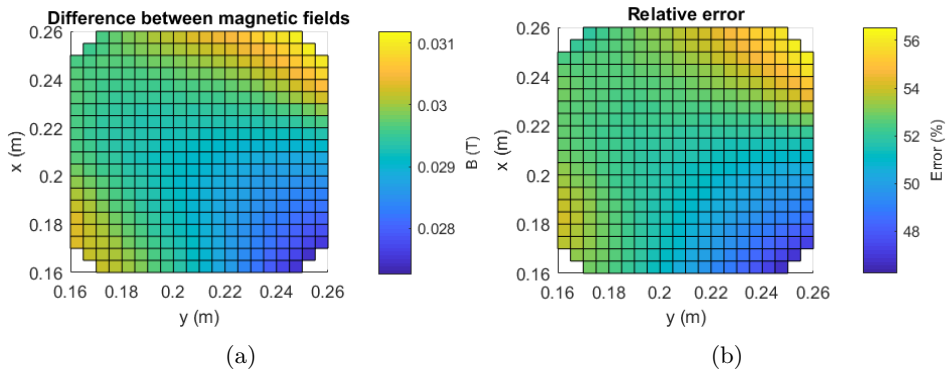

Figure 25: a) The difference between the simulated magnetic field and the measured field for the cylinder of four rings with the inner gradient and shimming rings in T. b) The error in the field relative to the measured magnetic field for the magnet cylinder in percentages.

The difference between the measured and the simulated magnetic field of the cylinder is quite significant. The average error of the field is 52%. Furthermore, it can be observed that the relative error, Figure 25b, has an offset.
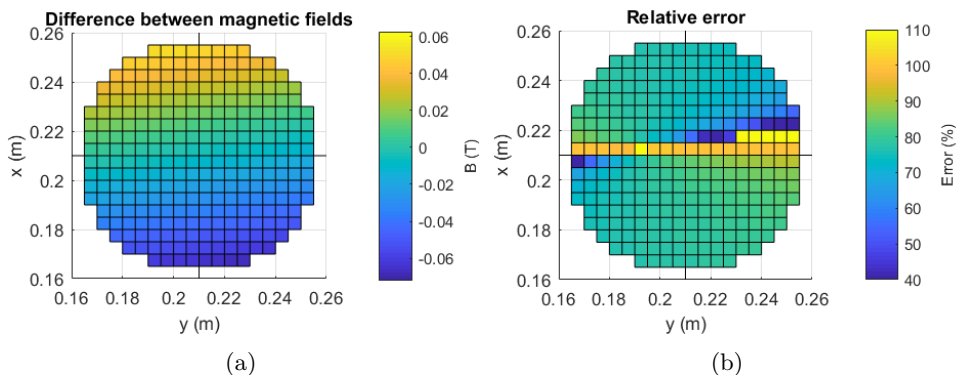

Figure 26: a) The difference between the simulated magnetic field and the measured field for the outer gradient ring in T. b) The error in the field relative to the measured magnetic field for the outer gradient ring in percentages.

As can be observed, the measured magnetic field of the outer gradient ring, Figure 19, has a much higher field strength than the simulated field, Figure 16. The mean error of the field is 80%.

These differences between simulations and reality are huge. Some of these differences are caused by the method of simulating. In the simulation, not cube magnets are used, but a complete ring is magnetized. In order to correct for this the field is also calculated with a correction factor as can be seen in (16):

$$B_{rec,cor} = B_{rec}\frac{V_{cube}}{V_{ring}}. \tag{16}$$

This correction factor makes a huge difference in the magnetic field of the cylinder ring as can be seen in Figure 27. This makes sense, since when using a ring, the magnetized volume is more than when only magnetizing cubes in the ring.
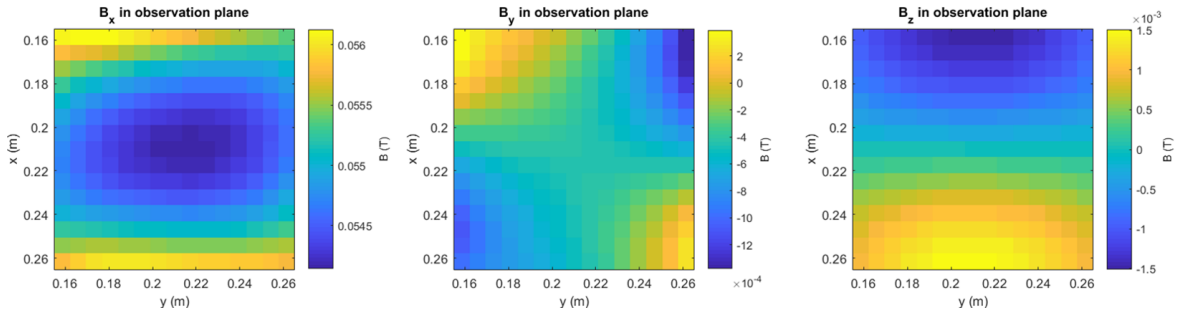

Figure 27: Corrected simulated magnetic field in the middle of the cylinder generated by the four first order Halbach rings, the inner gradient ring and the inner shimming rings. On the left, the *x*-component of the magnetic field is shown, in the middle, the *y*-component of the magnetic field is shown and on the right, the *z*-component of the magnetic field is shown.

In comparison, the difference between this field and the measured field is much lower than before, as can be seen in Figure 28. Now, the mean error in the magnetic field is 3.0%.
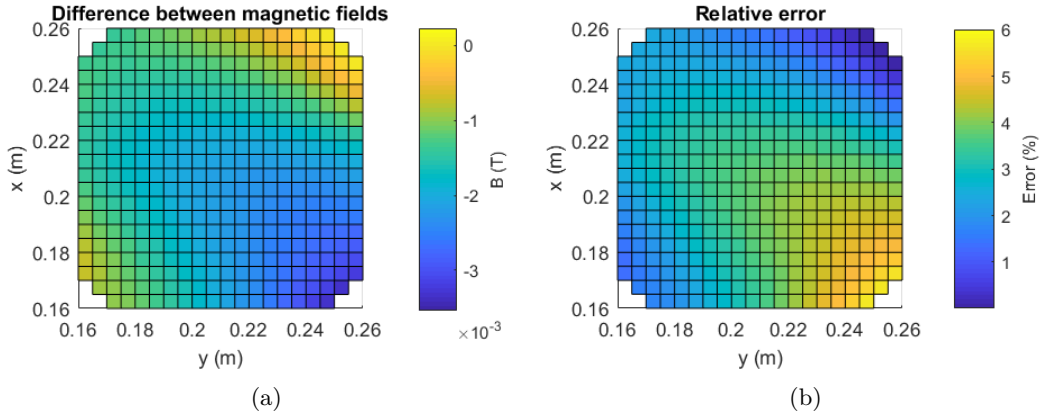
Figure 28: a) The difference between the simulated magnetic field and the measured field for the cylinder rings with the implemented shimming and gradient rings in T after the volume correction. b) The error in the field relative to the measured magnetic field for cylinder rings with the implemented shimming and gradient rings in percentages after the volume correction has been applied.

For the outer gradient, however, the volume correction does not change the magnetic field a lot, this

can be seen in the Figures 29 and 30.

Figure 29: Corrected simulated magnetic field in the middle of the outer gradient ring in T. On the left, the **x**-component of the magnetic field is shown, in the middle, the **y**-component of the magnetic field is shown and on the right, the **z**-component of the magnetic field is shown.

The average error in the field is in this case 79%, this is not much lower than the 80% from before the correction. This is explainable since the ring pieces in the simulated ring are already smaller since the ring has to be divided into 36 parts instead of the 24 for the four cylinder rings.
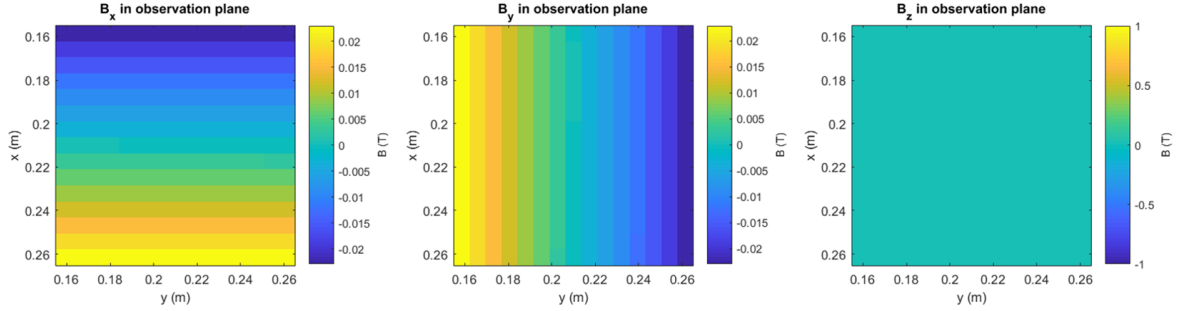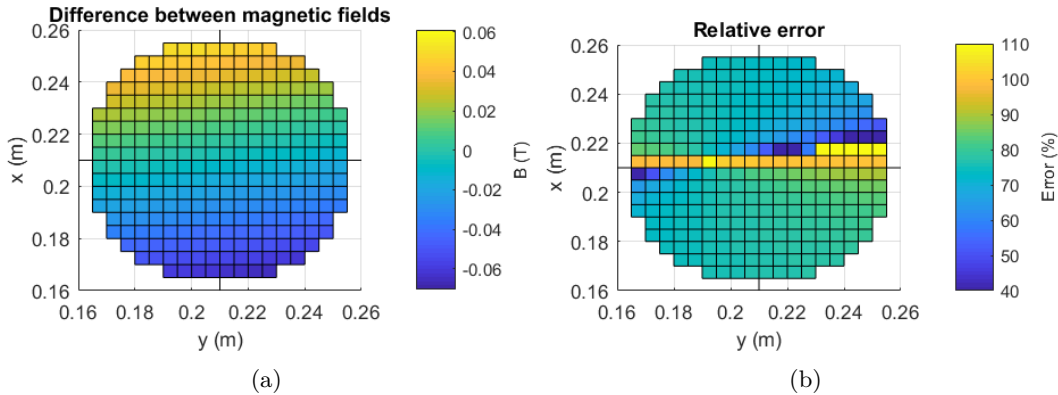

Figure 30: a) The difference between the simulated magnetic field and the measured field in T for the outer gradient ring after the volume correction. b) The error in percentages in the field relative to the measured magnetic field for the outer gradient ring after the volume correction.

The simulation after the volume correction still has a very large error. The error that is made looks like a scaling error since almost everywhere the measured field is around 4 times as large as the simulated field, the error is almost everywhere the same, Figure 30b. So, for the gradient ring, the difference lies somewhere else.

Other influences that have a smaller impact and that among other things cause the error in the corrected magnetic field of the cylinder are that there are uncertainties in the magnetizations of all the magnets. As well in the direction of the magnets as in the strength there is uncertainty. The strength of the magnetic remanence is between 1.45 and 1.48 T. In the simulations the mean of this interval, 1.465 T, is used, but there will be magnets that do have a slightly different remanence. However, this difference does not have a huge impact on the error between the fields. When using a B_r of 1.45 T, respectively 1.48 T, gives a mean error in the simulated gradient field of a bit higher than 80%, respectively a bit lower than 80%.

Furthermore, in the simulation, the direction of the magnetization is in the Halbach orientation, but

the orientation of the magnetization in the magnets might be a bit different.

Besides that, in the simulation the assumption is made that the influence that the magnets have on each others remanences is negligible, in reality, this could make a difference. The difference caused in the outer gradient ring might be a bit larger than in the magnet cylinder, since in the outer gradient ring, the magnets are placed closer to each other.

Furthermore, there is also the uncertainty of the measured magnetic field caused by the measuring machine, 1% of DC reading and +/- 10 counts with 1 count is 1×10^{-5} T, [16]. Since there is no DC reading, this uncertainty is +/- 1×10^{-4} T, which again is almost negligible compared to the differences between the measured and the simulated fields.

7.2 Optimization results

Several optimizations are done. Firstly, the Genetic Algorithm using one Halbach orientation with magnets having two options, being present in that Halbach orientation, or not being present at all. Secondly, the quasi-Newton Algorithm that is a continuous optimization algorithm for the orientation that the magnets have.

The results from the Genetic Algorithm show that only a few magnets already cause a field that is in field strength high enough for the gradient field. Since adding more magnets would increase the error for the field, many magnets are left out, such that for the first order Halbach optimization not even one magnet is present. Thus, it can be deducted from this that the magnets used for the outer gradient ring are probably much too strong for their application.

The results from the quasi-Newton Algorithm show that entirely different ring configurations can generate magnetic fields with a similar error relative to the desired magnetic field. Thus, this implies that there are many local minima in this optimization problem.

In both optimizations, the errors of the magnetic field the optimized rings generate are quite high, around the 30%. Since the algorithms give the magnetizations that would generate a field as close to the desired gradient field as possible, this suggests that the magnets used are not feasible for this desired gradient field.

All of these optimizations are done using a wrong desired magnetic field for the outer gradient ring since the volume correction was not taken into account, Figure 20b. In Figure 31, the corrected desired magnetic field for the outer gradient ring is given. This field can be found using the over all desired magnetic field 20a and subtracting the corrected magnetic field for the cylinder with inner shimming and gradient rings from that field, Figure 27.
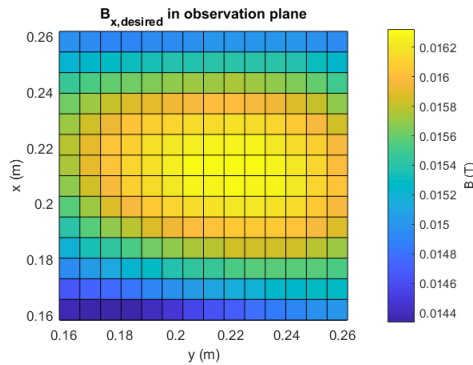

Figure 31: The new desired magnetic field in T for the outer gradient ring after the volume correction is applied to the magnet cylinder of four rings with the inner shimming and gradient rings.

7.3   Further optimizations and research

Since the optimizations in Chapter 6: Optimizations are all generated with a wrong desired magnetic field, the outcomes are not that useful. Thus, in this section a few optimizations will be repeated in order to check the results of the optimizations when using the corrected desired magnetic field.

First, again the Genetic Algorithm is used. Using the first order Halbach magnet configuration, now the mean relative error in the optimized field is 8.3%, with the best run giving an error of 7.8%. For the second Halbach order, this gives an average error of 51%, with the best run also giving an error of 51%, there is no significant difference between these errors. All the optimizations done using the second order Halbach configuration converge to the same optimum. As for the third order, again the difference between the best run and the other optimization runs is not significant, both have a relative error of 33%. The best optimizations are done using the fourth order with a mean relative error of 36%, the most optimal result also had an error of 36%. The best over all optimizations using the corrected rings gives that the first Halbach order should be used in order to obtain a result that resembles the desired magnetic field most. These results are shown in Figure 32.
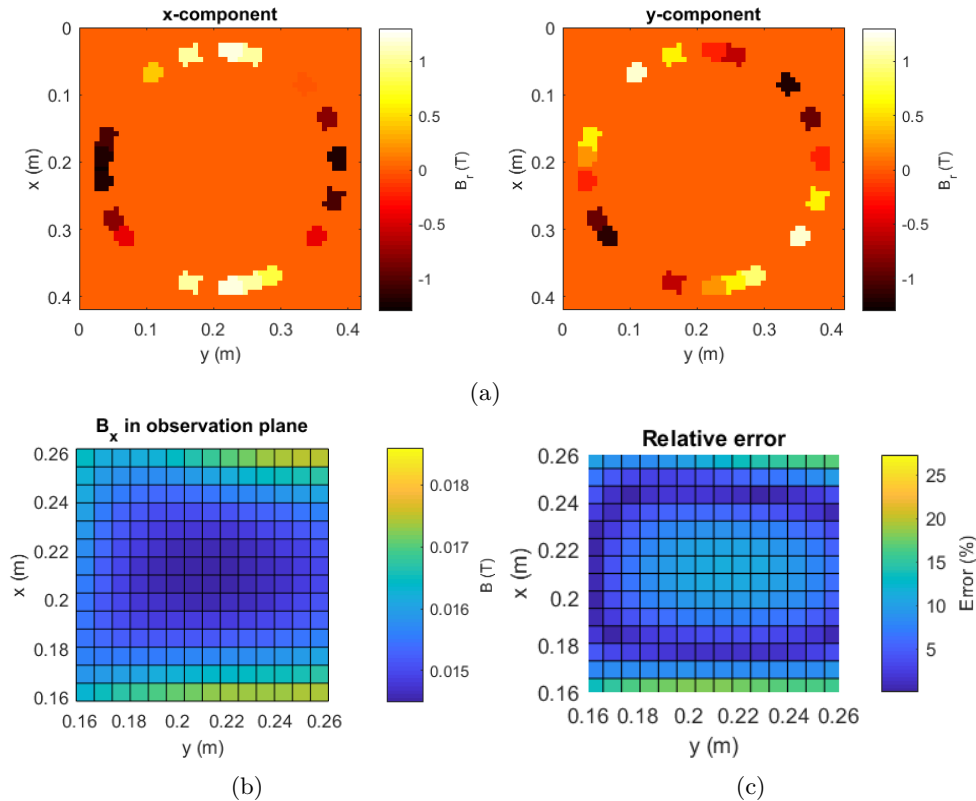

(a)

(b)   (c)

Figure 32: a) The magnetization in the x- and y-direction for the outer gradient ring for the optimized magnetic field using the Genetic Algorithm and a first order Halbach orientation on the outer gradient ring with the volume correction taken into account. b) The resulting magnetic field in the x-direction. c) The relative error in the resulting magnetic field in the x-direction.

All the first order Halbach optimizations using the volume correction show a similar result. The magnetization, Figure 32a, shows that the first Halbach order is used around the ring, but not all magnets are used. This also implies that magnets with a smaller magnet strength should be used. They probably should be put in the first order Halbach configuration, also since this.

Furthermore, also the quasi-Newton Algorithm is used in order to see what this algorithm gives using the volume correction factor. The total of the algorithm runs have an average relative error of 33%. The best run has a mean relative error of 32%. The results of this run are shown in Figure 33. It can be observed that also the continuous algorithm gives as a solution a first order Halbach resembling magnetization configuration.
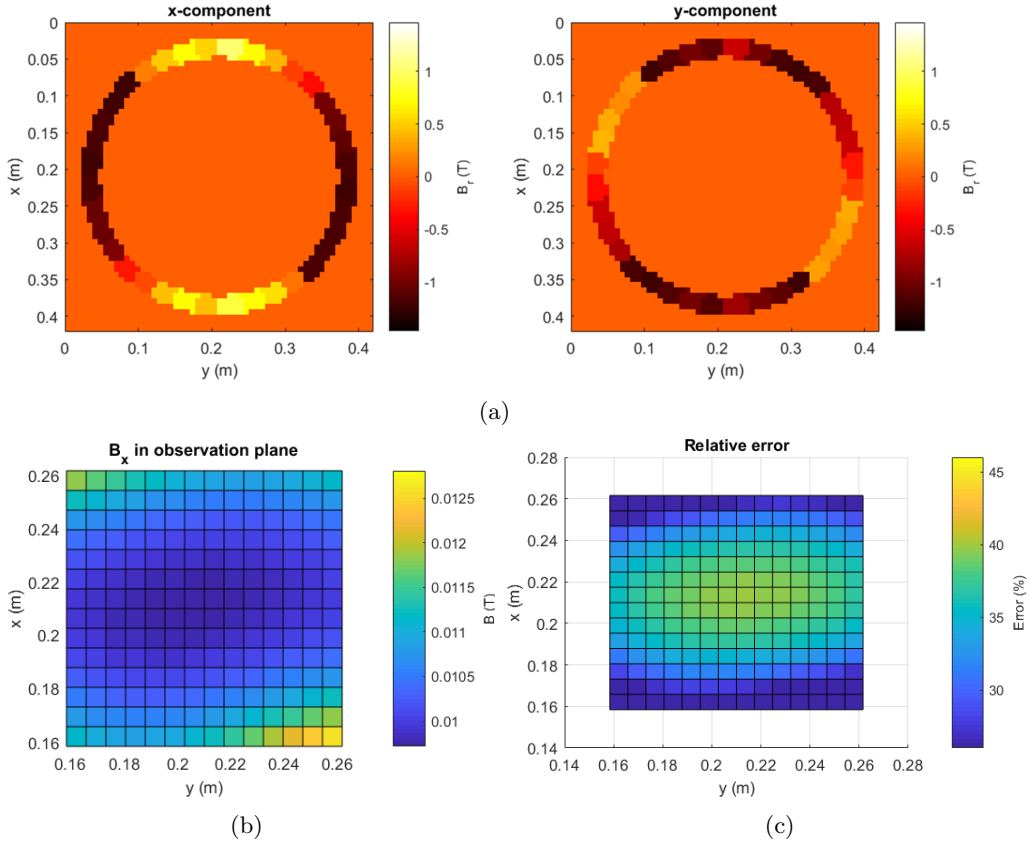

Figure 33: a) The magnetization in the x- and y-direction for the outer gradient ring for the optimized magnetic field using the quasi-Newton method with the volume correction factor taken into account. b) The resulting magnetic field in the x-direction. c) The error in the resulting magnetic field in the x-direction.

Thus, a direction for future research: to determine which size or strength magnets are needed for the gradient ring in order to be able to give a magnetic field that resembles the desired magnetic field more than what is reached in this research. A brief search in this direction is done. The Genetic Algorithm is used in order to optimize the orientation of the magnets for another magnet strength. The rare-earth NdFeB magnet N35 with its residual flux densities: 1.19 ± 0.02 T, [13], is used. For the size of the magnets the size of the current magnets in the outer gradient ring, a 1-inch cube, is taken. However, when running the Genetic Algorithm, this does not give better results than before, again the relative error is around the 8%. But for the continuous fminunc algorithm this will make a difference, since there all magnets are present by definition.

Furthermore, what would probably help is to take into account more orientations for the magnets in the discrete optimization. Now, every time the Genetic Algorithm is run using one configuration for the magnets. This is done for several configurations, but it could be useful to do more in depth research into this. This would give a more complete search for the optimal the gradient ring.

8   Conclusion

The main goal of this bachelor final project of the Delft University of Technology is to answer the question: 'How should the magnetic cubes in the outer gradient ring of a certain magnet cylinder be arranged in order to obtain a desired magnetic field inside the cylinder?'.

It can be concluded from the research done that the initial 1-inch N52 NdFeB outer gradient ring is not suitable at all for generating the desired gradient field. The gradient it generates is much too high. The discrete Genetic Algorithm does give a result that resembles the desired magnetic field for the gradient ring quite well. The mean relative error of the generated magnetic field of the outer gradient ring then is 8.3%. For the best optimization run the first order Halbach order is used, giving an error of 7.8%. Using the continuous optimization algorithm with all the magnets present does not give a very good result. This is because the magnets used are too strong to generate the desired magnetic field when all the magnets are present. Thus, the fminunc algorithm gives a mean relative error in the field of 33% with the best run giving a mean relative error of 32%. The solutions for the gradient ring using the GA are sparse, implying that the field the magnets generate is too strong for giving the desired magnetic field.

A way of improving the outer gradient ring could be optimizing the ring for the desired magnetic field with magnets with a different magnetic remanence or a different size in the fminunc algorithm. Weaker or smaller magnets would probably be more suitable to use if the gradient ring should be completely filled.
For the Genetic Algorithm reducing the magnet size or strength does not improve the optimization results. Thus, further research could be done into taking into account more directions per magnet in the optimizations. Now only one orientation is taken into account per optimization. It would give more insight if more directions are taken into account in one optimization run.

References

[1] J. P. Heida and B. J. Otter, "NVZ Brancherapport ziekenhuizen: Vergelijking Europa", The Hague, The Netherlands, Jul. 2012.

[2] G. I. Ogbole, A. O. Adeyomoye, A. Badu-Peprah, Y. Mensah, and D. A. Nzeh, "Survey of magnetic resonance imaging availability in West Africa", *The Pan African Medical Journal*, Jul. 2018. DOI: `10.11604/pamj.2018.30.240.14000`.

[3] M. Dewan, et al., "Global hydrocephalus epidemiology and incidence: systematic review and meta-analysis", *Journal of Neurosurgery*, Apr. 2018. DOI: `10.3171/2017.10.JNS17439`.

[4] LUMC - Leids Universitair Medisch Centrum, 2018.

[5] P. Blümler, "Permanent Magnet System for MRI with Constant Gradient mechanically adjustable in Direction and Strength", *Concepts in Magnetic Resonance Part B: Magnetic Resonance Engineering*, Feb. 2016. DOI: `10.1002/cmr.b.21320`.

[6] D. J. Griffiths, *Introduction to Electrodynamics*, 4th edition. Cambridge, UK: Cambridge University Press, 2017.

[7] M. L. de Leeuw den Bouter, *Image reconstruction in low-field MRI: A super-resolution approach*, Delft, The Netherlands, Jun. 2017.

[8] Z.-P. Liang and P. C. Lauterbur, *Principles of Magnetic Resonance Imaging: A Signal Processing Perspective*. Wiley-IEEE Press, 2000.

[9] A. Berger, "Magnetic resonance imaging", *British Medical Journal*, Jan. 2002. DOI: `10.1136/bmj.324.7328.35`.

[10] A. D. Elster. (2018). Questions and Answers in MRI, [Online]. Available: `http://mriquestions.com/what-is-spin.html`. (accessed: 11.07.2019).

[11] J. Lilja, *Multi subject study of motor sensory function in rat brain using fMRI*, Stockholm, Sweden, 2005.

[12] A. D. Elster. (2018). Questions and Answers in MRI, [Online]. Available: `https://www.mriquestions.com/does-precession--nmr.html`. (accessed: 17.07.2019).

[13] K&J Magnetics, *Specifications*, Pipersville, USA. [Online]. Available: `https://www.kjmagnetics.com/specs.asp`, (accessed: 20.07.2019).

[14] Supermagnete, *Data sheet article W-12-N - Technical data and application safety*, Germany, Nov. 2011. [Online]. Available: `https://www.supermagnete.de/eng/data_sheet_W-12-N.pdf`, (accessed: 20.07.2019).

[15] ——, *Data sheet article W-05-N - Technical data and application safety*, Germany, Nov. 2011. [Online]. Available: `https://www.supermagnete.nl/data_sheet_W-05-N.pdf`, (accessed: 20.07.2019).

[16] AlphaLab, Inc., *Gaussmeter Model GM2 Instructions*, West Salt Lake City, USA. [Online]. Available: `https://www.alphalabinc.com/product/gm2/`.

[17] H. Han, et al., "Open Source 3D Multipurpose Measurement System with Submillimetre Fidelity and First Application in Magnetic Resonance", *Nature - Scientific Reports*, Oct. 2017. DOI: `10.1038/s41598-017-13824-z`.

[18] C.Z.Cooley, et al., "Design of Sparse Halbach Magnet Arrays for Portable MRI Using a Genetic Algorithm", *IEEE Transactions on Magnetics*, vol. 54, 1 Jan. 2018. DOI: `10.1109/TMAG.2017.2751001`.

[19] A. Chipperfield and P. Fleming, "The MATLAB Genetic Algorithm Toolbox", 1995.

[20] A. Chipperfield, P. Fleming, H. Pohlheim, and C. Fonseca, *Genetic Algorithm Toolbox - For Use with MATLAB, User's Guide*, version Version 1.2, University of Sheffield, 1994.

[21]   MathWorks. (2019). Unconstrained Nonlinear Optimization Algorithms, [Online]. Available: `https://nl.mathworks.com/help/optim/ug/unconstrained-nonlinear-optimization-algorithms.html`. (accessed: 23.07.2019).

[22]   E. W. Weisstein. (2019). Hessian, MathWorld–A Wolfram Web Resource, [Online]. Available: `http://mathworld.wolfram.com/Hessian.html`. (accessed: 23.07.2019).

[23]   R. Remis, *Magnetic Field Theory - notes*, 2016.

A   Appendix

A.1   Calculation of the magnetic flux density of a magnetized object, [23]

Starting from a three-dimensional vacuum space without any current densities and a static situation of the magnet, Gauss's law for magnetism becomes:

$$\nabla \times \mathbf{H} = \mathbf{0}, \tag{17}$$

$$\nabla \cdot \mathbf{B} = \mathbf{0}, \tag{18}$$

where $\mathbf{H}$ is the magnetic field strength in $\mathrm{A\,m^{-1}}$ and $\mathbf{B}$ is the magnetic flux density in T.
Now, the aim is to find the magnetic flux density $\mathbf{B}$ due to the presence of permanent magnets outside these magnets. Suppose the permanent magnet occupies a bounded domain $\mathcal{D}$ and it is characterized by a permanent magnetization $\mathbf{M}$ that is independent of the magnetic flux density. Since the magnetic flux density is divergence-free, it can also be expressed in the following way:

$$\mathbf{B} = \nabla \times \mathbf{A}. \tag{19}$$

Here $\mathbf{A}$ is the magnetic vector potential in $\mathrm{V\,s/m}$. This potential is required to satisfy the following condition:

$$\nabla \cdot \mathbf{A} = \mathbf{0}. \tag{20}$$

(20) is called the Coulomb gauge.

Taking the curl of (19) gives

$$\nabla \times \mathbf{B} = \nabla \times (\nabla \times \mathbf{A}) = \nabla\nabla \cdot \mathbf{A} = \nabla^2\mathbf{A} = \nabla^2\mathbf{A}, \tag{21}$$

where (20) is taken into account. Thus it can easily be observed that

$$\nabla^2\mathbf{A} = -\nabla \times \mathbf{B}. \tag{22}$$

Outside the magnet, the following constitutive relation holds:

$$\mathbf{B} = \mu_0\mathbf{H}, \tag{23}$$

with μ_0 is the magnetic permeability in vacuum.
Thus combining Equations 22, 23 and 17 gives

$$\nabla^2\mathbf{A}(\mathbf{r}) = -\mu_0\nabla \times \mathbf{H}(\mathbf{r}) = \mathbf{0}, \tag{24}$$

for $\mathbf{r} \notin \mathcal{D}$.
Inside the magnet, not (23), but (25) holds.

$$\mathbf{B}(\mathbf{r}) = \mu_0\mathbf{H}(\mathbf{r}) + \mu_0\mathbf{M}(\mathbf{r}), \tag{25}$$

with $\mathbf{M}$ is the magnetization at $\mathbf{r} \in \mathcal{D}$. Thus here when combining (22), (25) and (17), this gives:

$$\nabla^2\mathbf{A}(\mathbf{r}) = -\mu_0\nabla \times \mathbf{H}(\mathbf{r}) - \mu_0\nabla \times \mathbf{M} = -\mu_0\nabla \times \mathbf{M}. \tag{26}$$

Using (24) and (26) and Green's function, with a bit of calculating, the following vector potential is found:

$$\mathbf{A}(\mathbf{r}) = -\frac{\mu_0}{4\pi}\nabla \times \int \frac{\mathbf{M}(\mathbf{r}')}{|\mathbf{r} - \mathbf{r}'|}d\tau'. \tag{27}$$

Here the integral is over the volume of the magnetic material and the potential is given in the entire 3D-space.

Now, (19) can be applied and writing out gives:

$$\mathbf{B}(\mathbf{r}) = \frac{\mu_0}{4\pi} \boldsymbol{\nabla}\boldsymbol{\nabla} \cdot \int \frac{\mathbf{M}(\mathbf{r'})}{|\mathbf{r} - \mathbf{r'}|} d\tau'. \tag{28}$$

This is the magnetic flux density outside the magnet.

It can be seen that the observation vector $\mathbf{r}$ does not belong to the integration domain ($\mathbf{r'}$ does belong to the integration domain). Thus, the order of integration and differentiation can be interchanged,

$$\mathbf{B}(\mathbf{r}) = \frac{\mu_0}{4\pi} \int \boldsymbol{\nabla}\boldsymbol{\nabla} \cdot \frac{\mathbf{M}(\mathbf{r'})}{|\mathbf{r} - \mathbf{r'}|} d\tau'. \tag{29}$$

Then with the gradient-divergence operation this finally gives the following equation:

$$\mathbf{B}(\mathbf{r}) = \frac{\mu_0}{4\pi} \int \frac{3\mathbf{q}(\mathbf{r}, \mathbf{r'})(\mathbf{q}(\mathbf{r}, \mathbf{r'}) \cdot \mathbf{M}(\mathbf{r'})) - \mathbf{M}(\mathbf{r'})}{|\mathbf{r} - \mathbf{r'}|^3} d\tau', \tag{30}$$

with $\mathbf{q}(\mathbf{r}, \mathbf{r'}) = \frac{\mathbf{r} - \mathbf{r'}}{|\mathbf{r} - \mathbf{r'}|}$ with $\mathbf{r}$ being outside the magnet and $\mathbf{r'}$ being within the magnet.